FAM210B is an erythropoietin target and regulates erythroid heme synthesis by controlling mitochondrial iron import and ferrochelatase activity

Received for publication, March 5, 2018, and in revised form, September 11, 2018 Published, Papers in Press, October 26, 2018, DOI 10.1074/jbc.RA118.002742

Yvette Y. Yien,[a,b1] Jiahai Shi,[c2] Caiyong Chen,[b3] Jesmine T. M. Cheung,[d] Anthony S. Grillo,[e] Rishna Shrestha,[f] Liangtao Li,[f] Xuedi Zhang,[a] Martin D. Kafina,[b4] Paul D. Kingsley,[g] Matthew J. King,[b5] Julien Ablain,[h] Hojun Li,[c] Leonard I. Zon,[h,i] James Palis,[g] Martin D. Burke,[e] Daniel E. Bauer,[h,i] Stuart H. Orkin,[h,i] Carla M. Koehler,[d] John D. Phillips,[j] Jerry Kaplan,[f] Diane M. Ward,[f] Harvey F. Lodish,[c] and Barry H. Paw[†b,h,i]

From the [a]Department of Biological Sciences, University of Delaware, Newark, Delaware 19716, the [b]Division of Hematology, Brigham and Women's Hospital, Harvard Medical School, Boston, Massachusetts 02115, the [c]Whitehead Institute and Department of Biology, Massachusetts Institute of Technology, Cambridge, Massachusetts 02139, the [d]Department of Chemistry and Biochemistry, UCLA, Los Angeles, California 90095, the [e]Department of Chemistry and Biochemistry, University of Illinois at Urbana-Champaign, Urbana, Illinois 61801, the [f]Department of Pathology, University of Utah School of Medicine, Salt Lake City, Utah 84112, the [g]Center for Pediatric Biomedical Research, Department of Pediatrics, University of Rochester Medical Center, Rochester, New York 14642, the [h]Division of Hematology-Oncology, Boston Children's Hospital, Harvard Medical School, Boston, Massachusetts 02115, the [i]Department of Pediatric Oncology, Dana-Farber Cancer Institute, Harvard Medical School, Boston, Massachusetts 02115, and the [j]Division of Hematology and Hematologic Malignancy, University of Utah School of Medicine, Salt Lake City, Utah 84112

Edited by Joel M. Gottesfeld

Erythropoietin (EPO) signaling is critical to many processes essential to terminal erythropoiesis. Despite the centrality of iron metabolism to erythropoiesis, the mechanisms by which EPO regulates iron status are not well-understood. To this end, here we profiled gene expression in EPO-treated 32D pro-B cells and developing fetal liver erythroid cells to identify additional iron regulatory genes. We determined that FAM210B, a mitochondrial inner-membrane protein, is essential for hemoglobinization, proliferation, and enucleation during terminal erythroid maturation. *Fam210b* deficiency led to defects in mitochondrial iron uptake, heme synthesis, and iron–sulfur cluster formation. These defects were corrected with a lipid-soluble, small-molecule iron transporter, hinokitiol, in *Fam210b*-deficient murine erythroid cells and zebrafish morphants. Genetic complementation experiments revealed that FAM210B is not a mitochondrial iron transporter but is required for adequate mitochondrial iron import to sustain heme synthesis and iron–sulfur cluster formation during erythroid differentiation. FAM210B was also required for maximal ferrochelatase activity in differentiating erythroid cells. We propose that FAM210B functions as an adaptor protein that facilitates the formation of an oligomeric mitochondrial iron transport complex, required for the increase in iron acquisition for heme synthesis during terminal erythropoiesis. Collectively, our results reveal a critical mechanism by which EPO signaling regulates terminal erythropoiesis and iron metabolism.

The glycoprotein cytokine erythropoietin (EPO)[6] plays a major role in regulation of erythroid survival and differentiation by activation of signaling pathways via EPO receptor binding (1). Among its roles is the up-regulation of erythroferrone to suppress hepcidin to increase availability of iron during stress erythropoiesis (2, 3). However, the physiological functions of EPO in the regulation of iron metabolism are largely uncharacterized.

Iron, as an ion, and in the forms of iron–sulfur [Fe-S] clusters and heme, is an essential cofactor for redox reactions in diverse

This work was supported by March of Dimes Foundation Grant 6-FY09-289 (to B. H. P.); the Cooley's Anemia Foundation (to C. C. and Y. Y. Y.); the National Science Foundation (to A. S. G.); National Institutes of Health Grants F32 DK098866, R03 DK118307, and K01 DK106156 (to Y. Y. Y.), K08 DK093705 (to D. E. B.), K99CA20146 (to J. A.), R01 DK020503 and U54 DK083909 (to J. D. P.), R01 GM073981 and R01 GM61721 (to C. M. K.), R01 DK052830 and DK030534 (to D. M. W.), R01 HL116364 (to J. P.), R01 GM118185 (to M. D. B.), R01 DK070838 (to B. H. P.), P01 HL032262 (to H. F. L., S. H. O., L. I. Z., and B. H. P.); and the University of Delaware Biological Sciences Undergraduate Summer Scholar award (to X. Z.). The authors declare that they have no conflicts of interest with the contents of this article. The content is solely the responsibility of the authors and does not necessarily represent the official views of the National Institutes of Health.

The microarray data for this study were deposited to the NCBI Gene Expression Omnibus (GEO) database under GEO accession number GSE113657.

[†] Deceased December 28, 2017.

This article contains Figs. S1–S3.

[1] To whom correspondence should be addressed: Dept. of Biological Sciences, University of Delaware, Newark, DE 19716. Tel.: 302-831-6685; E-mail: yyien@udel.edu.

[2] Present address: City University of Hong Kong, Hong Kong, China.

[3] Present address: College of Life Sciences, Zhejiang University, Hangzhou 310058, China.

[4] Present address: Dept. of Medicine, St. George's University School of Medicine, St. George, Grenada, West Indies.

[5] Present address: University of Texas Health Science Center, San Antonio, TX 78229.

[6] The abbreviations used are: EPO, erythropoietin; ICM, intermediate cell mass; PMSF, phenylmethylsulfonyl fluoride; LCR, locus control region; PPIX, protoporphyrinogen IX; DP, deuteroporphyrin IX; qRT, quantitative RT; GAPDH, glyceraldehyde-3-phosphate dehydrogenase; P, pellet; S, soluble; MEL, murine erythroleukemia; DFO, desferrioxamine; ALAS, 5-aminolevulinate synthase; IRE, iron-responsive element; MEF, mouse embryonic fibroblast; BSA, bovine serum albumin; ICP, inductively coupled plasma; hpf, hours post-fertilization.

cellular processes, such as dopamine synthesis, oxygen transport, mitochondrial respiration, xenobiotic metabolism, and maintenance of the circadian rhythm (4–9). However, the majority of iron in the body is used by erythroid cells to synthesize hemoglobin (10, 11). Free iron is highly toxic because of its ability to generate free radicals through the Fenton reaction. Although iron is obtained from outside the cell and is required for reactions that take place in membrane-bound organelles, cellular membranes are not permeable to iron. Organisms have therefore evolved sophisticated mechanisms to efficiently transport iron across membranes (11, 12). In the majority of vertebrate cells, iron is mainly obtained through the transferrin-mediated pathway (13, 14), which is SNX3- and SEC15L1-dependent for efficient transferrin receptor recycling in erythroid cells (15, 16). In the plasma, each transferrin molecule binds two Fe^{3+} ions. Iron-bound transferrin interacts with transferrin receptor on the cell surface. This complex is internalized via clathrin-mediated endocytosis. Within the acidified endosome, Fe^{3+} is reduced to Fe^{2+} by STEAP proteins (17). Fe^{2+} is exported from the endosome by endosomal DMT1 (18–20) and may enter the mitochondrial intermembrane space via DMT1, which is localized on the mitochondrial outer membrane (21). Iron that is used for heme synthesis or iron–sulfur [Fe-S] clusters is imported into the mitochondrial matrix by the mitochondrial iron importer mitoferrins 1 and/or 2 (MFRN1/SLC25A37 or MFRN2/SLC25A28) (22–24). In developing red cells, the stabilization of MFRN1 by ABCB10 (25) is a mechanism by which the cell ensures efficient iron import for its utilization in hemoglobin synthesis (26). However, the Δ*mrs3*Δ*mrs4* yeast strain that is deficient in the mitoferrins only exhibited a partial defect in mitochondrial iron import. This suggests the existence of other mitochondrial iron importers (27, 28) or of auxiliary mechanisms that augment iron import to compensate for the genetic insufficiency of an iron transporter.

We identified potential EPO-regulated iron transport genes by microarray analysis of the EPO-treated, EpoR-expressing pro-B cell line, 32D, and we compared EPO-responsive genes to genes that were up-regulated during terminal erythropoiesis. One candidate gene, *Fam210b (C20orf120)*, encoded a protein containing an N-terminal mitochondrial-targeting sequence. *Fam210b* was previously described to be a target of the erythroid transcription factor, GATA1, which encoded a mitochondrial-localized protein (29) that regulates mitochondrial metabolism in nonerythroid cells (30). In this study, we decided to interrogate the role of *Fam210b* in erythroid physiology. *Fam210b* expression is highly up-regulated during terminal erythropoiesis, which requires large quantities of iron. Loss-of-function studies in zebrafish embryos, primary murine fetal liver cells, and Friend murine erythroleukemia (MEL) cell lines show that FAM210B is required specifically to maintain the massive quantities of mitochondrial iron necessary for heme synthesis during terminal erythropoiesis. Although FAM210B is not an iron transporter *per se*, it interacts with terminal heme synthesis enzymes to form an oligomeric complex. Collectively, our data reveal that FAM210B plays a critical role as an adaptor protein in a mitochondrial iron import oligomeric complex. FAM210B is essential for integration of the rapid iron import with a high rate of porphyrin synthesis that supports hemoglobinization during terminal erythropoiesis. This study describes a novel mechanism by EPO governs enucleation and cellular proliferation, processes underlying terminal erythropoiesis, by its control of mitochondrial iron uptake and heme biosynthesis.

Results

Fam210b is an immediate early target of EPO during terminal erythroid differentiation

Maturing erythroid cells acquire large quantities of exogenous iron to keep pace with the enormous demands of hemoglobin production (31, 32). To determine how EPO regulates iron transport, we identified genes up-regulated by EPO in the EpoR-expressing pro-B cell line, 32D (33). Cells were cultured in media without erythropoietin for 6 h prior to treatment with Epo (0.5 units/ml) for 2 h before harvesting. We analyzed global gene expression in control and EPO-treated murine 32D cells by microarray analysis. To determine which EPO targets could also be required for erythroid terminal differentiation, we compared the EPO-responsive genes in 32D cells with genes that were enriched in $TER119^+$ cells (34), which comprise the terminally differentiating erythroid cell population. We found that *Fam210b* expression was enriched in both datasets (Fig. 1*A*). To determine whether *Fam210b* was an EPO early response gene, a parallel experiment was set up in which 32D cells were treated with cycloheximide (10 μg/ml) 30 min prior to EPO stimulation to inhibit protein translation (35, 36). We observed that *Fam210b* expression was induced by EPO treatment, suggesting that *Fam210b* is an EPO target. The up-regulation of *Fam210b* expression persisted during cycloheximide treatment, indicating that *Fam210b* is an EPO early-response gene (Fig. 1*B*). The increase in *Fam210b* mRNA levels in response to EPO stimulation and during terminal differentiation translated to increases in the FAM210B protein. Interestingly, FAM210B protein was also up-regulated in the presence of cycloheximide, indicating that EPO increases the post-translational stability of FAM210B (Fig. 1*C*).

To determine how *Fam210b* is developmentally regulated, we performed RNA sequencing (RNAseq) on transcripts from murine fetal liver erythroid cells (34) that were sorted into fractions corresponding to their stage of maturation (R1–R5) (15, 37–39). *Fam210b* expression was up-regulated during maturation from R2 to R3, which corresponds to the developmental shift from $TER119^-$ to $TER119^+$ expression. This expression pattern was similar to that of genes involved in heme synthesis and iron import, such as *Fech* and *Tfrc* (Fig. 1*D*), and it is consistent with the enrichment of *Fam210b* in the $TER119^+$ population (Fig. 1*A*). FAM210B protein expression in the R2–R3 transition was recapitulated at the protein level (Fig. 1*E*). Consistent with this, FAM210B protein levels increase during *in vitro* differentiation of primary fetal liver erythroid cells (Fig. 1*F*) and in DMSO-induced terminal differentiation of MEL cells (Fig. 1*G*). The increases in protein expression are coordinated with α-globin (HBA) (Fig. 1*F*), TFRC, and FECH (Fig. 1*G*), which are critical to erythroid differentiation, heme, and hemoglobin synthesis, suggesting that FAM210B plays an essential role in erythroid development. Although the

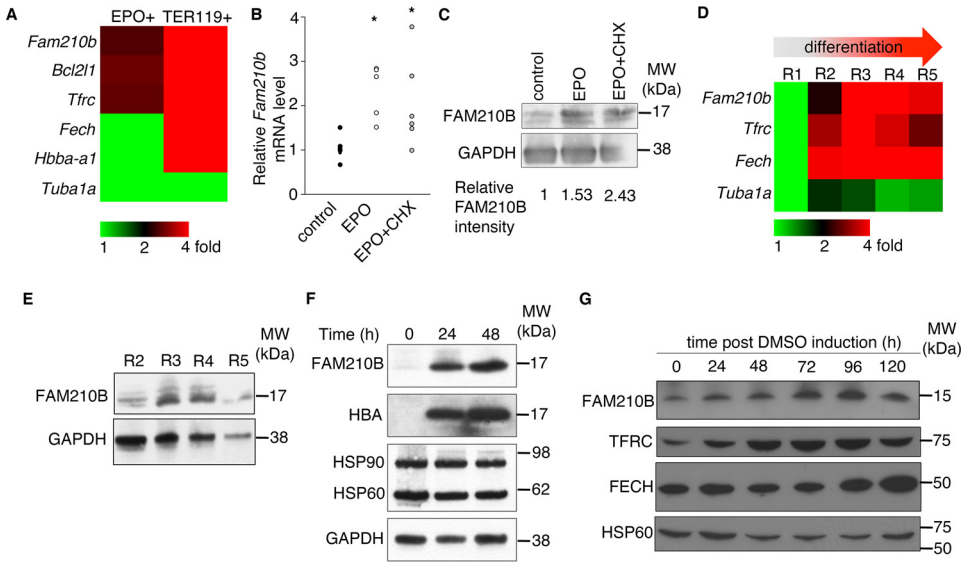

Figure 1. *Fam210b* is an EPO early response gene and is induced in terminally differentiating erythroid cells. *A*, microarray analysis of EPO-treated 32D pro-B cells shows that *Fam210b* is an EPO-responsive gene that is also highly enriched in the terminally differentiating TER119$^+$ population of fetal liver erythroid cells (34). *B*, qRT-PCR demonstrates that Epo treatment of the EpoR-expressing pro-B cell line, 32D, up-regulated expression of *Fam210b* mRNA. This up-regulation persists in the presence of cycloheximide (*CHX*), an inhibitor of protein translation, demonstrating that *Fam210b* is an EPO early response gene $n = 6$. *, $p < 0.05$, Student's *t* test. *C*, FAM210B protein levels are up-regulated in response to EPO treatment of the EpoR-expressing 32D pro-B cell line. The increase in protein levels persist with cycloheximide treatment, indicating increased stability. Changes in FAM210B protein expression normalized to GAPDH are quantitated relative to control levels. *D*, RNAseq analysis of primary murine fetal liver cells sorted according to TER119 and CD71 (*R1–R5*) expression demonstrates up-regulation of *Fam210b* during the R2–R3 transition. *E*, this up-regulation is recapitulated by Western blot analysis of FAM210B protein expression. *F*, FAM210B protein expression is up-regulated during *in vitro* differentiation of primary fetal liver cells. *G*, FAM210B protein is induced upon terminal differentiation of MEL cells in parallel with genes required for heme synthesis, *TFRC* and *FECH*. *, $p < 0.05$, Student *t* test.

expression of iron homeostasis genes is sometimes regulated by intracellular iron status via iron-regulatory proteins, IRP1 and IRP2 (13), we found that this was not the case for FAM210B (Fig. S1).

In situ hybridization of E12.5 murine embryos (performed as described (40)) indicated that *Fam210b* mRNA is enriched in the murine fetal liver at E12.5, the site of definitive erythropoiesis (Fig. 2*A*). In the adult mouse, *Fam210b* is enriched in the bone marrow, liver, and skeletal muscle, which are tissues that require large amounts of heme for synthesis of hemoproteins, and the testis, where iron plays an essential role in spermatogenesis (Fig. 2*B*) (41). In contrast to *gata1, fam210b* mRNA is maternally expressed in the developing zebrafish embryo. At 24 hpf, expression of *fam210b* mRNA is restricted to neuronal tissue and the intermediate cell mass (ICM), which is the site of primitive erythropoiesis in teleosts. *fam210b* is not expressed in *cloche* embryos (42, 43), which have defective blood and vascular progenitors. Conversely, *fam210b* expression is expanded in *dino* embryos. In *dino* embryos, the tail is expanded at the expense of the head (44). The tail is also the site of the ICM, which is the site of primitive hematopoiesis in the zebrafish. These zebrafish therefore have expanded blood due to their ventralized phenotype. The enrichment of *fam210b* in early hematopoietic tissues in zebrafish embryos, its absence in mutants that do not make hematopoietic progenitors, and the expansion of its expression in the *dino* mutants, which have an expanded ICM, indicate that *fam210b* expression depends on hematopoietic specification (Fig. 2*C*). At 72 hpf, *fam210b* expression persists in neural tissue and the liver (Fig. 2*D*), which are tissues that require large amounts of iron for their function (8, 13).

Fam210b is required for erythropoiesis in vivo

To determine the biological function of *fam210b*, we injected antisense morpholinos to knock down its expression in developing zebrafish embryos. As *fam210b* is highly expressed in terminally differentiating erythroid cells (Fig. 1, *A* and *B*), we assayed heme synthesis in morphant embryos by *o*-dianisidine staining as a measure of terminal erythropoiesis. Compared with the controls, *fam210b* morphants have significantly decreased heme staining, indicative of their anemia (Fig. 3*A*). We quantitated the erythropoietic defect by flow cytometry analysis of GFP$^+$ cells in morphant *Tg*(*globin-LCR:eGFP*) transgenic zebrafish, which express GFP under the control of a globin locus control region (LCR) enhancer, restricting *GFP* expression to the erythroid lineage (45). Morphant embryos exhibited decreased erythropoiesis at 24- and 48-hpf, highlighting the importance of *fam210b* in erythropoiesis (Fig. 3*B*).

To determine whether *Fam210b* was required for mammalian erythropoiesis, we knocked down *Fam210b* in primary fetal liver erythroid cells with shRNA (Fig. 3*C*). *Fam210b* knockdown caused a reduction in hemoglobinization (Fig. 3*D*), which was partially ameliorated by co-expression of human *FAM210B* (Fig. 3*E*), indicating the functional orthology between the human and mouse *FAM210B* genes. Knockdown of FAM210B caused defects both in cell proliferation (Fig. 3*F*) and in enucleation (Fig. 3*G*), indicating its additional function in erythroid maturation. The independent validations of the erythroid defect in *Fam210b* knockdown zebrafish and murine models indicate that the role of FAM210B in terminal erythroid maturation is highly conserved in vertebrates. In higher vertebrates, continuous FAM210B expression in the erythron is required

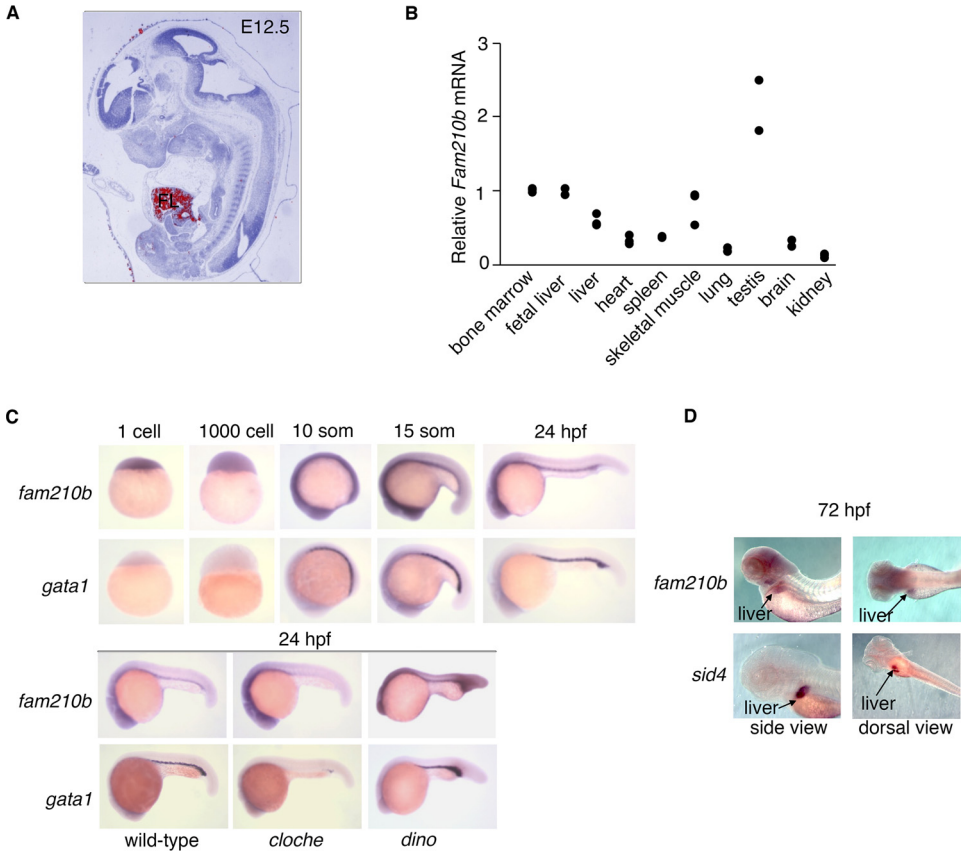

Figure 2. Expression of *Fam210b* is enriched in vertebrate tissues with high heme content. *A, Fam210b* expression (*red* pseudocolor) is enriched in the murine fetal liver (*FL*) at E12.5. *B,* in murine tissues, *Fam210b* expression is enriched in the bone marrow and fetal liver (erythroid), adult liver, skeletal muscle, and testis, all of which require high levels of iron for their function. *C,* zebrafish *fam210b* is maternally expressed during early embryonic development. At 24 hpf, *fam210b* expression is enriched in neural tissue and the intermediate cell mass, the site of primitive hematopoiesis (*top*). The expression of *fam210b* in the ICM is abolished in *cloche* embryos, which do not form hematopoietic or vascular tissue. In contrast, *fam210b* expression in the intermediate cell mass is expanded in *dino* embryos, which exhibit a ventralized phenotype (*bottom*), paralleling the increased expression of erythroid *gata1*. *D,* at 72 hpf, *fam210b* expression persists in the neural tissue and is enriched in the liver, delineated by *sid4* expression. $n = 3$.

for optimal erythroid cell proliferation, maturation, hemoglobinization, and enucleation.

Fam210b is localized to the mitochondrial inner membrane

To delineate the cellular mechanism by which FAM210B regulates erythropoiesis, we transfected *fam210b-GFP* into HEK293T cells and examined its subcellular localization. Fam210b contains three hydrophobic stretches of ~21 amino acids, suggesting that FAM210B is an integral membrane protein. Confocal immunofluorescence microscopy revealed that FAM210B-GFP co-localized with COX4, a mitochondrial resident protein (Fig. 4*A*). Subcellular fractionation and Western blot analysis of primary fetal liver cells confirmed that FAM210B specifically co-localized with HSP60, a mitochondrial resident protein (Fig. 4*B*).

We carried out further localization studies in MEL cells stably expressing *Fam210b* to determine the sub-mitochondrial localization of FAM210B. To determine the localization of FAM210B in the mitochondrial outer membrane, purified mitochondria were treated with proteinase K, followed by centrifugation to separate the intact mitochondria (P) from soluble proteins (S) (Fig. 4*C*). Immunoblotting showed that TOMM20, an outer membrane protein with a large cytosolic domain, was degraded upon protease treatment, whereas FAM210B and control proteins YME1 (intermembrane space) and PreP (matrix) were intact. FAM210B is therefore not an outer mitochondrial membrane protein.

The mitochondria were then subjected to osmotic shock to determine whether FAM210B was in the intermembrane space or matrix (Fig. 4*C*). Mitoplasts, which contain the inner membrane and matrix components and intermembrane space/outer membrane components that stick to the mitoplasts, were recovered by centrifugation (P), whereas soluble proteins (S) remained in the supernatant. The mitoplasts were subsequently treated with a low dose of proteinase K to degrade proteins that were in the intermembrane space. FAM210B and PreP were resistant to protease digestion, whereas intermembrane space protein YME1 was degraded as expected. As a control for proteinase K activity, the mitoplasts were treated with Triton X-100, thereby releasing membrane-bound proteins into the supernatant and exposing digestion sites to enzymatic digestion. The addition of proteinase K to the Triton X-100 detergent-treated samples resulted in complete degradation, with the exception of PreP that has a tightly folded domain that is resistant to the low doses of proteinase K. These data suggested that FAM210B was bound to the mitochondrial inner membrane.

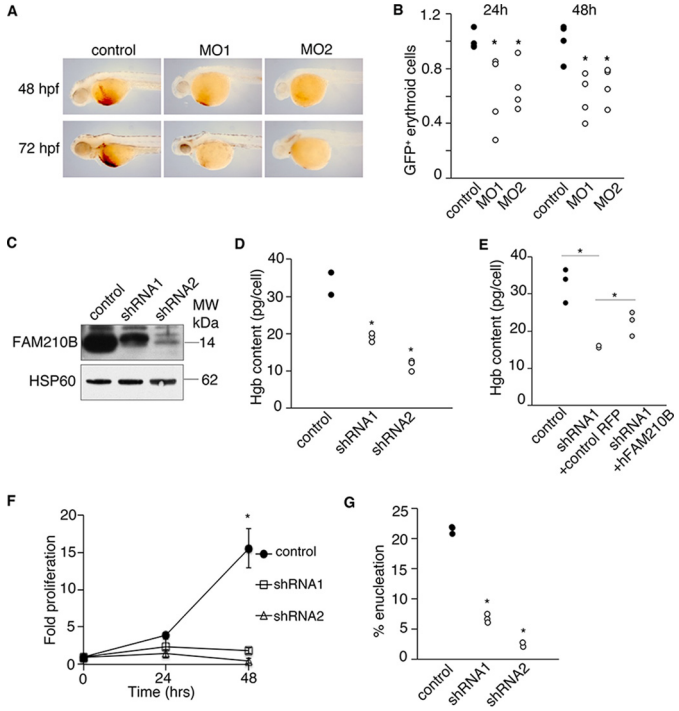

Figure 3. Fam210b is continuously required for terminal erythroid differentiation. *A,* knockdown of *fam210b* in zebrafish embryos with two independent antisense morpholinos caused a defect in erythroid hemoglobinization. *B, Tg*(*globin LCR:eGFP*), *fam210b* morphant zebrafish exhibited a decrease in GFP$^+$ erythroid cells, indicating defective erythropoiesis, $n = 4$; *, p value < 0.05 Student's t test. *C,* shRNA-mediated knockdown of *Fam210b* in primary fetal liver cells decreased FAM210B protein expression. *D, Fam210b* knockdown primary fetal liver cells had a decrease in hemoglobin content. *E,* hemoglobinization defect in murine *Fam210b* knockdown cells is complemented by human *FAM210B*. *F, Fam210b* knockdown in primary fetal liver cells caused a cell proliferation defect. *G, Fam210b* knockdown caused an enucleation defect, indicative of erythroid maturation arrest. $n = 3$, *, p value < 0.05 Student's t test.

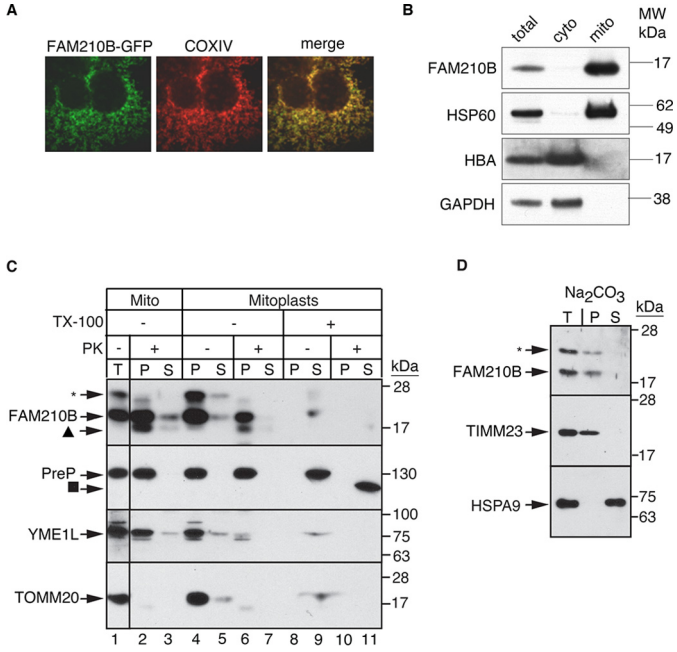

Figure 4. FAM210B localizes to the mitochondrial inner membrane. *A,* confocal fluorescence microscopy of exogenously expressed FAM210B-GFP (*green*) in HEK293T cells indicated that FAM210B co-localized with COXIV (*red*), a mitochondrial resident protein. The overlap is indicated in the *merge panel* (*yellow*). *B,* subcellular fractionation of primary fetal liver cells showed that FAM210B co-sedimented with HSP60 (mitochondrial) but not with HBA and GAPDH (cytoplasmic), indicating its mitochondrial localization. *C,* isolated mitochondria (*Mito, T*; *lanes 1–3*) purified from a MEL cell line stably expressing mouse *Fam210b*, was treated with proteinase K, which degraded outer membrane proteins (TOMM20) but not intermembrane space proteins (YME1L) or matrix (PreP) proteins (*lane 2*). Inner mitochondrial proteins, which were impervious to proteinase K treatment, (*P*) were separated from S proteins by centrifugation. FAM210B co-sedimented with the pellet fraction (*lane 2*). Mitoplasts (*lanes 4–11*) were generated by subjecting intact mitochondria to osmotic shock, exposing inner membrane and intermembrane space proteins to proteinase K digestion. Mitoplasts were centrifuged to separate the soluble proteins from the mitoplast pellet. Proteinase K treatment degraded a fraction of FAM210B (*lane 6*) and completely degraded YME1L but not PreP, suggesting that at least a fraction of FAM210B was situated in the mitochondrial inner membrane or intermembrane space. Triton X-100 (*TX-100*) treatment liberated FAM210B, PreP, and YME1L from the pellet into the soluble fraction (*lane 9*). These solubilized proteins were digested by proteinase K, demonstrating specificity of assay (*lane 10*). The *asterisk* marks a nonspecific band that was detected with the mouse FAM210B antibody; the *triangle* marks a likely FAM210B degradation product; and the *square* marks a core of PreP that is tightly folded and resistant to protease treatment. *D,* to determine whether FAM210B was an integral inner-membrane protein, isolated mitochondria (*T*) were analyzed by carbonate extraction. P and S fractions were analyzed by immunoblotting for FAM210B. The blot was probed for TIMM23 as an integral membrane protein control and mortalin as a soluble protein control. An *asterisk* marks nonspecific bands detected by the FAM210B antibody.

To rigorously confirm that this was the case, mitochondria were subjected to sodium carbonate extraction (46), followed by centrifugation, to separate membrane proteins (pellet, P) from soluble (S) proteins (Fig. 4*D*). FAM210B and membrane-bound TIMM23 were recovered in the pellet, whereas soluble matrix-localized HSPA9 (mortalin) was released in the supernatant. Thus, FAM210B is an integral membrane protein residing in the inner membrane. The collective data indicate that FAM210B is integrated in the inner membrane, and any soluble domains are likely facing the matrix, because protease addition during osmotic shock did not markedly degrade the full-length protein. A smaller fragment, which was sub-stoichiometric, was detected in the pellet (Fig. 4*C*, *marked with a triangle*), which may indicate that the N or C terminus is facing the intermembrane space and is digested by protease that may have leaked into the intermembrane space. The smaller fragment sediments with the pellet, suggesting that the segment of FAM210B that is exposed to the protease is tightly associated with the membrane.

FAM210B facilitates mitochondrial iron import during terminal erythropoiesis

To determine the biochemical function of FAM210B in heme synthesis, we generated *Fam210b*-deficient MEL cell lines by CRISPR/Cas9 genome editing (Fig. 5*A*). Metabolic ^{55}Fe-labeling revealed that undifferentiated *Fam210b*$^{-/-}$ MEL cells had normal rates of heme synthesis and iron uptake compared with WT controls (Fig. 5, *B* and *C*). However, when MEL cells were chemically induced to differentiate, heme synthesis and iron uptake in *Fam210b*$^{-/-}$ MEL cells was significantly impaired (Fig. 5, *D* and *E*). The heme synthesis defect in *Fam210b*$^{-/-}$ MEL cells was due to a deficiency in mitochondrial iron acquisition (Fig. 5, *F* and *G*). As FAM210B is required for optimal mitochondrial iron uptake, we assayed the activity of mitochondrial aconitase (EC 4.2.1.3) in FAM210B$^{-/-}$ cells. Mitochondrial aconitase activity is sensitive to mitochondrial iron deficiency (47) caused by defects in mitochondrial iron

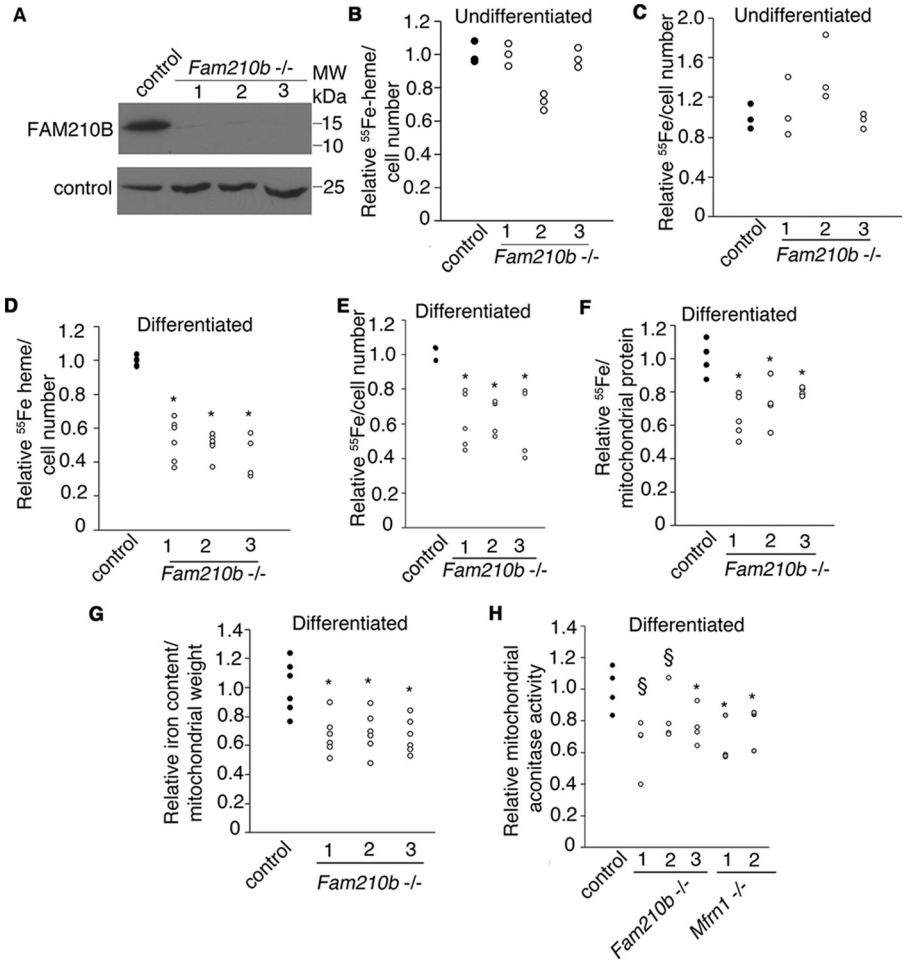

Figure 5. Fam210b is required for heme synthesis by facilitating mitochondrial iron import. *A, Fam210b*$^{-/-}$ MEL cell lines generated by CRISPR/Cas9 expressed no detectable FAM210B protein. *B,* ^{55}Fe metabolic labeling showed that *undifferentiated Fam210b*$^{-/-}$ MEL cell clones did not cause changes in heme synthesis ($n = 3$) or iron uptake ($n = 3$) (*C*). *D, differentiated Fam210b* knockout MEL cells exhibited defective heme synthesis ($n = 6$). *E,* iron uptake ($n = 5$). *F,* mitochondria from differentiated *Fam210b* knockout cells had decreased ^{55}Fe-transferrin uptake ($n = 5$). *G,* ICP-MS demonstrated that mitochondria from *Fam210b* knockout cells had a decrease in total iron ($n = 6$). *H,* mitochondrial aconitase activity, which depends on [Fe-S] cluster synthesis, is decreased in *Fam210b*$^{-/-}$ cells indicating a defect in mitochondrial iron acquisition. *Mfrn1*$^{-/-}$ MEL clones served as controls for mitochondrial iron deficiency ($n = 4$). *, $p < 0.05$; §, $p < 0.1$ Student's *t* test. All data are normalized to WT controls.

transport, and this is reflected by the aconitase defect in *Mfrn1*$^{-/-}$ MEL cells (Fig. 5*H*) (23, 28). *Fam210b*$^{-/-}$ cells had a decrease in mitochondrial aconitase activity that is comparable with *Mfrn1*$^{-/-}$ cells, indicating that it plays a critical role in mitochondrial iron metabolism.

The heme synthesis (Fig. 6*A*) and iron transport (Fig. 6*B*) defects in *Fam210b*$^{-/-}$ MEL cells were functionally complemented to the level of WT cells by hinokitiol (CAS 499-44-5; ChEBI: 10447), a natural product that binds iron and autonomously transports both Fe(II) and Fe(III) across lipid membranes to bypass defects in iron transport (48). Iron-hinokitiol functionally complemented the erythropoietic defect in *fam210b* morphant zebrafish embryos (Fig. 6*C*), demonstrating that the primary role of FAM210B is to facilitate mitochondrial delivery of iron for the synthesis of heme and [Fe-S] clusters in the developing erythroid cell. C2-deoxyhinokitiol, which does not bind or transport iron, did not chemically complement the anemia in *Fam210b*$^{-/-}$ cells (Fig. 6, *A* and *B*), indicating that the ability of the iron-hinokitiol to rescue heme synthesis was directly dependent on the ability of hinokitiol to chelate and transport iron across membranes (48). The specificity of the functional complementation is further demonstrated by the restoration of both ^{55}Fe and ^{55}Fe-heme only in cells defective for iron transport, such as the *Dmt1* knockdown cell line (19, 20), but not in cells with a porphyrin transport defect, such as the *Tmem14c* CRISPR cell line (38).

HPLC analysis of protoporphyrinogen IX (PPIX) content in differentiating *Fam210b*$^{-/-}$ cells indicated that FAM210B was not required for synthesis of the tetrapyrrole ring in the mitochondria (Fig. S2*A*). This was further confirmed by the inability of deuteroporphyrin IX (DP), a PPIX analog that can chemically complement porphyrin synthesis defects (38), to rescue heme synthesis in *Fam210b*$^{-/-}$ cells (Fig. S2*B*).

To exclude the possibility that the heme defect in FAM210B deficiency was caused by a lesion in mitochondrial biogenesis or physiology, we stained control and *Fam210b*$^{-/-}$ cells with Mitotracker dye and analyzed mitochondrial staining by flow cytometry. The percentage of Mitotracker-positive cells and average Mitotracker dye staining did not differ between control and *Fam210b*$^{-/-}$ cells, indicating that *Fam210b* deficiency did not cause defects in cell survival (Fig. S2*C*), mitochondrial membrane potential, and mitochondrial mass (Fig. S2*D*).

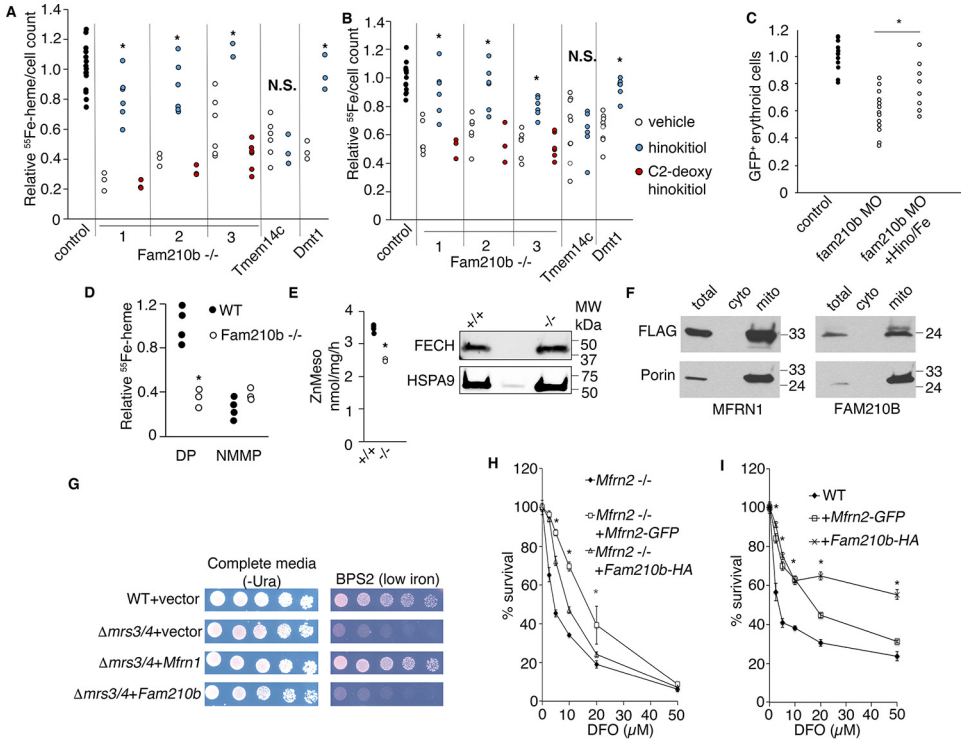

Figure 6. Fam210B increases the kinetics of mitochondrial iron import in differentiating MEL cells by functioning as an auxiliary factor. *A,* ^{55}Fe metabolic labeling confirmed a decrease in heme synthesis in differentiating *Fam210b* (CRISPR1–3), *Tmem14c,* and *Dmt1* deficient MEL cells (*black bars*). The addition of hinokitiol, a lipid-soluble iron carrier (*white bars*), restored heme synthesis in *Fam210b*- and *Dmt1*-deficient cells, but not *Tmem14c*-deficient cells. C2-deoxyhinokitiol, which does not chelate iron, did not complement heme synthesis in the *Fam210b* knockout cells (*gray bars*) ($n = 6$). *B,* ^{55}Fe metabolic labeling confirmed an iron uptake defect in differentiating *Fam210b*-, *Tmem14c*-, and *Dmt1*-deficient cells (*black bars*). The iron uptake defect in *Fam210b*- and *Dmt1*-deficient cells was chemically complemented by hinokitiol (*white bars*). Hinokitiol did not rescue iron uptake in *Tmem14c*-deficient cells, which have a porphyrin synthesis defect. C2-deoxyhinokitiol did not rescue the iron deficiency in *Fam210b*$^{-/-}$ cells (*gray bars*) ($n = 6$). *C,* treatment of *fam210b* morphant zebrafish embryos (*MO*) with iron citrate and hinokitiol (*MO + Hino/Fe*) rescued their anemia ($n = 8$). *D,* FECH activity was measured in intact mitochondria isolated from WT and *Fam210b*$^{-/-}$ MEL cells, using ^{55}Fe and DP as substrates. FECH activity in *Fam210b*$^{-/-}$ mitochondria was ~1/3 that of WT controls. Both WT and *Fam210b*$^{-/-}$ mitochondria had very little measurable FECH activity when NMMP was used as a substrate ($n = 4$). *E,* FECH activity was measured in isolated mitochondria from WT and *Fam210b*$^{-/-}$ MEL cells that were treated with detergent and disrupted by sonication, allowing access of reaction substrates to FECH in the absence of intact membranes. FECH activity was decreased in *Fam210b*$^{-/-}$ mitochondria, but not to the extent of intact mitochondria ($n = 3$). *F,* FLAG-tagged MFRN1 and FAM210B co-localized with porin in Δ*mrs3/4* yeast, indicating correct mitochondrial localization. *G, Mfrn1* expression complemented the growth defect of Δ*mrs3/4* yeast in low-iron media, whereas *Fam210b* expression did not. *H,* survival of *Mfrn2*$^{-/-}$ fibroblasts in DFO is significantly complemented by expression of *Mfrn2-GFP*, but less so by expression of *Fam210b-HA* ($n = 3$). *I,* expression of *Fam210b-HA* and *Mfrn2-GFP* in WT fibroblasts increase cell survival in the presence of DFO, with *Fam210b* overexpression possessing a protective effect over a larger dose range than *Mfrn2-GFP*. Mean ± S.E., $n = 3$, *, $p < 0.05$; §, $p < 0.1$ Student's *t* test. *N.S.*, not significant.

FAM210b is not a direct mitochondrial iron carrier in vertebrate erythroblasts

To determine whether FAM210B functions as a mitochondrial iron importer or whether it played a role in regulation of FECH, we carried out an *in vitro* heme synthesis assay to compare the amount of iron transported across the mitochondrial membrane to synthesize deuteroheme (49). ^{55}Fe and DP were added to isolated mitochondria from WT and *Fam210b*$^{-/-}$ MEL cells. DP was added in excess. As DP is lipid-soluble, any differences in the synthesis of ^{55}Fe-DP are caused by alterations in FECH activity or iron transport across the mitochondrial membrane. In the absence of FAM210B, *in vitro* heme synthesis decreased to background levels comparable with cells treated with NMMP, a PPIX analog that inhibits FECH and cannot be metallated (Fig. 6*D*) (50). These data suggested that FAM210B is required for either iron import or heme synthesis. To determine which was the case, we performed a FECH activity assay as described (81). Using this method, cells are disrupted by sonication and treatment with Tween 20 detergent, allowing the substrates, mesoporphyrin IX, and zinc access to FECH without the need to cross membranes. FECH activity is measured by quantification of the product zinc-mesoporphyrin IX by HPLC. In the absence of a mitochondrial membrane, we observed that *Fam210b*$^{-/-}$ cells exhibited a decrease in FECH activity (Fig. 6*E*, *left*). This was not attributable to a decrease in FECH protein levels (Fig. 6*E*, *right*). Based on Fig. 6, *D* and *E*, FAM210B is required for optimal FECH activity in erythroid cells. However, we observed that the decrease in FECH activity was far less significant when membranes were disrupted (Fig. 6*E*) compared with when the mitochondrial membrane was intact (Fig. 6*D*). We concluded that FAM210B is required both for full activation of FECH but also plays a role in facilitating iron transport across the mitochondrial membrane for heme synthesis.

To determine whether FAM210B is a *bona fide* iron transporter, we expressed epitope-tagged *Fam210* or *Mfrn* in the Δ*mrs3*Δ*mrs4* yeast strain (denoted as Δ*mrs3/4*), deficient in the Mfrn orthologs (23), or in *Mfrn2*$^{-/-}$ primary murine fibroblasts,[7] which are deficient in mitochondrial iron transporter

[7] D. M. Ward and J. Kaplan, unpublished data.

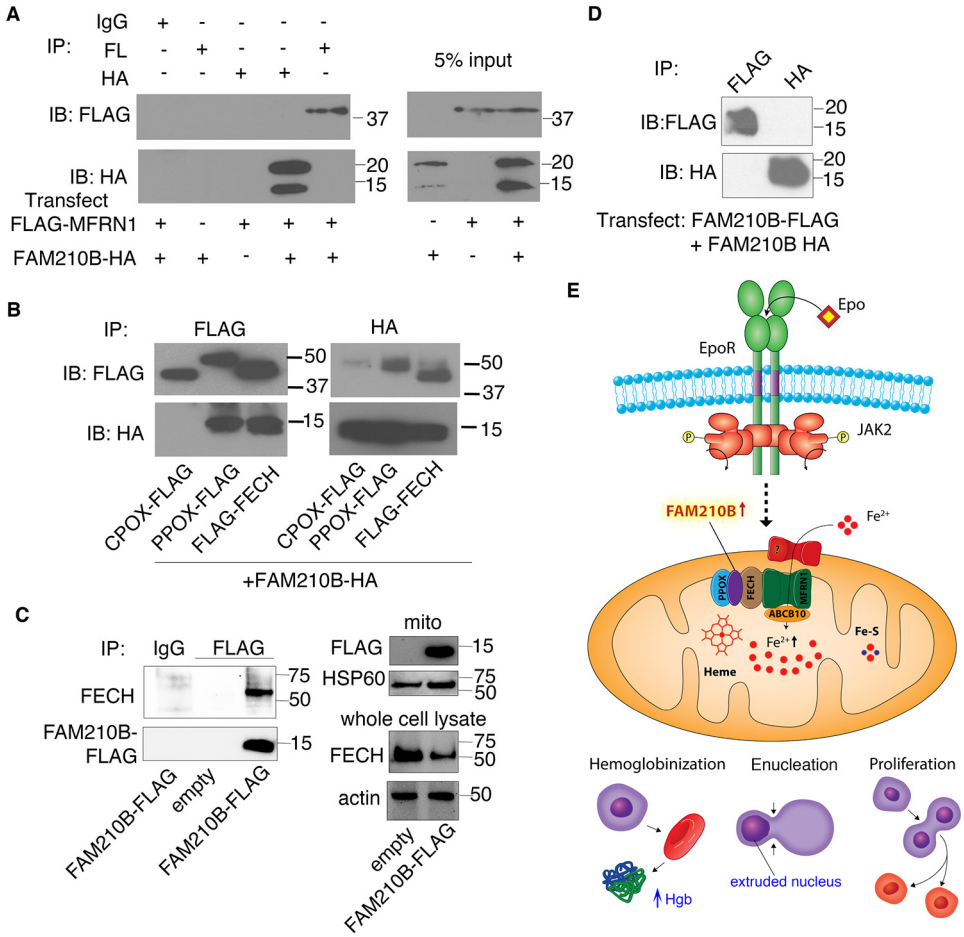

Figure 7. FAM210B directly interacts with terminal heme synthesis enzymes but does not with MFRN1 (Slc25a37). *A,* immunoprecipitation of co-expressed FAM210B-HA and FLAG-MFRN1 demonstrates FAM210B does not directly interact with MFRN1. *B,* FAM210B-HA interacts with the terminal enzymes of the heme synthesis pathway, PPOX and FECH, but not CPOX. MFRN1, CPOX, PPOX, and FECH are all localized to the mitochondrial inner membrane. *C,* immunoprecipitation of FAM-210B FLAG stably expressed in differentiating MEL cells shows that ectopically expressed FAM210B interacts with endogenous FECH. *D,* FAM210B-HA and FAM210B-FLAG do not interact, demonstrating that FAM210B does not homooligomerize. *E,* model of the role of FAM210B as an adaptor protein in an oligomeric complex with terminal heme enzymes, required for terminal erythropoiesis and mitochondrial iron importation.

Slc25a28 (22). Mouse FAM210B, with the N-terminal mitochondrial targeting propiece from Mrs3, properly targeted to the mitochondrial compartment in yeast (Fig. 6*F* and Fig. S3). Δ*mrs3/4* yeast exhibited iron auxotrophy when grown on iron-deficient media, which was genetically complemented by vertebrate *Mfrn1* but not *Fam210b* (Fig. 6*G*), suggesting that FAM210B does not directly function as a iron-solute carrier.

We next treated mouse embryonic fibroblasts from *Mfrn2*$^{-/-}$ with varying concentrations of desferrioxamine (DFO), an iron chelator, for 48 h. As cells require iron for basic cellular processes such as respiration, defects in cellular iron uptake and utilization would decrease cellular viability with DFO treatment. Conversely, increasing the expression of iron transporters would increase the efficiency of iron uptake and utilization in cells, resulting in increased survival. As expected, the expression of *Mfrn2-GFP* in *Mfrn2*$^{-/-}$ fibroblasts significantly improved cellular viability in DFO-treated cells (Fig. 6*H*). In contrast, *Fam210b* co-expression did not significantly enhance fibroblast viability above the basal control, demonstrating that *Fam210b* could not genetically complement *Mfrn2* deficiency (Fig. 6*H*). However, FAM210B significantly increases the survival of WT fibroblasts in a wide range of DFO concentrations beyond that of *Mfrn2-GFP* expression (Fig. 6*I*). As FAM210B augments iron import in WT but not in *Mfrn2*$^{-/-}$ MEFs, we propose that FAM210B increases the efficiency of mitochondrial iron import by an MFRN-dependent mechanism.

FAM210b is in an iron-import oligomeric complex to enhance heme synthesis

To further characterize the biochemical function of FAM210B in an oligomeric complex, we examined MFRN1 levels in *Fam210b*$^{-/-}$ MEL cells to determine whether *Fam210b* plays a role in *Mfrn1* stability analogous to ABCB10, as MFRN1 is the predominant erythroid mitochondrial iron transporter (22, 23, 25). MFRN1 protein levels were similar in control and *Fam210b*$^{-/-}$ mitochondria, indicating that FAM210B does not play a role in the maintenance of MFRN1 stability (Fig. S2*E*). Immunoprecipitation of FAM210B that was ectopically co-expressed with MFRN1 in HEK293T cells showed that FAM210B and MFRN1 do not interact (Fig. 7*A*). In contrast, we co-immunoprecipitated ectopically expressed FAM210B with PPOX and FECH (Fig. 7*B*), which are terminal enzymes in the heme synthesis pathway. As the ectopically expressed proteins are expressed at levels far higher than endogenous FAM210B, PPOX,

and FECH or potential bridging proteins that can mediate indirect interactions, it is likely that the physical interactions between FAM210B, PPOX, and FECH are direct. Notably, PPOX and FECH are in the same complex as MFRN1 (Chen *et al.* (26) and Medlock *et al.* (79)). The specificity of these protein–protein interactions is ensured by the lack of CPOX co-immunoprecipitation with FAM210B (Fig. 7*B*). To further determine whether FAM210B can interact with FECH at endogenous levels, we generated a MEL cell line that stably expressed FAM210B–FLAG. We immunoprecipitated FAM210B with FLAG antibodies in differentiating cells. Western blot analysis of the immunoprecipitated protein showed that FAM210B–FLAG interacted with endogenous FECH *in vivo* (Fig. 7*C*). FAM210B does not homooligomerize, as would be expected if FAM210B was a membrane-embedded solute carrier (Fig. 7*C*). Collectively, these results are consistent with a role for FAM210B as an auxiliary factor in an iron transport oligomeric complex that includes the terminal heme biosynthesis enzymes in the mitochondria. The intact oligomeric complex is essential for maintaining the high rate of mitochondrial iron import that is required to fulfill the demands for heme synthesis in maturing red cells.

Discussion

Our study demonstrates that FAM210B, a protein of previously unknown function, is required for mitochondrial iron import to support sustained synthesis of heme, iron–sulfur cluster, and hemoglobin during erythroid maturation. In addition, FAM210B regulates FECH enzyme activity. Our results are consistent with and extend the findings of a recent study identifying *Fam210b* as a GATA1 transcriptional target that is required for erythroid differentiation (29). Mitochondrial mass, membrane potential, and porphyrin levels are normal in *Fam210b*$^{-/-}$ cells, precluding a role for FAM210B in housekeeping mitochondrial homeostasis or tetrapyrrole synthesis, respectively. Although heme synthesis and iron import was decreased in *Fam210b*-deficient cells, we did not observe an accumulation in porphyrin, similar to the phenotype in *Mfrn1* deficiency (51, 52). This is attributable to impaired [Fe-S] cluster biosynthesis in *Fam210b*-deficient cells (Fig. 5*H*), which elevates IRP1 RNA binding and suppresses *Alas2* mRNA translation and porphyrin accumulation (52, 53).

FAM210B deficiency can be functionally complemented by the addition of hinokitiol, which acts as a small-molecule mimetic of iron transporters (48). However, *Fam210b* overexpression cannot genetically complement the iron transport defect in Δ*mrs3/4* yeast or *Mfrn2*$^{-/-}$ fibroblasts. We therefore conclude that the primary function of FAM210B is to facilitate mitochondrial iron import in differentiating erythroid cells by functioning as an auxiliary factor in promoting formation of an oligomeric iron–transport complex with terminal heme synthesis enzymes, thereby increasing the kinetics of mitochondrial iron import to keep pace with its cellular demands for heme. Our studies on FAM210B are the first to describe an EPO-induced mitochondrial chaperone that is tissue- and differentiation stage-specific, revealing a novel mechanism by which cells regulate intracellular iron metabolism. We previously identified a mitochondrial chaperone, CLPX, which facilitates the delivery of the vitamin B_6 cofactor required for the catalytic activity of ALAS, the enzyme that catalyzes the committed step of protoporphyrin synthesis (54). The oligomerization of MFRN1, ABCB10, and FECH integrates the efficient import of iron with the metallation of PPIX to form heme during erythroid maturation (26). We further note that the use of small molecules that autonomously perform protein-like functions as a distinct type of biological probe, as demonstrated herein with the transmembrane iron transporter hinokitiol, may be more widely applicable and have complementary strengths to other experimental approaches (48, 55).

Fam210b is transcriptionally activated by GATA-1 (29, 56), consistent with its expression in erythropoietic tissues. Iron chelation by DFO or iron supplementation by iron citrate did not cause changes in its steady-state protein expression, indicating that FAM210B is not regulated by cellular iron status (Fig. S1).

EPO regulates FAM210B expression both at the levels of mRNA transcription and protein stability, suggesting that FAM210B is an essential component of EPO's function and signaling in erythropoiesis. The up-regulation of *Fam210b* by EPO in EpoR-expressing 32D pro-B cells suggests that *Fam210b* is direct target of EPO. Although FAM210B is localized in the mitochondria, it is required for cellular processes that take place during terminal erythroid differentiation, such as proliferation, and finally enucleation. These data suggest a link between nuclear processes in terminal erythroid differentiation and mitochondrial iron metabolism and also demonstrate a novel mechanism by which EPO regulates the biology of terminal erythropoiesis via its regulation of cellular iron uptake.

Although published GWAS studies did not reveal any extant association between *FAM210B* mutations and hematologic traits (57–61), the profoundly anemic phenotype of the *fam210b* morphant embryos and the heme defects in primary murine fetal liver and in MEL cells predict that mutations in *FAM210B* may lead to hematologic and iron metabolism defects in humans. As *MFRN1* genetic or splicing defects have been shown to be modifiers of porphyria (62) or sideroblastic anemia (63), we predict that detailed genetic studies will reveal the function of *FAM210B* mutations in patients suffering from anemias and porphyrias of unknown etiology. As *Fam210b*$^{-/-}$ cells only exhibited heme and iron metabolism defects in differentiating erythroid cells, it is expected that *FAM210B* mutations will exhibit a phenotype specifically in the terminally differentiating erythroid cell population.

To adapt to their role as oxygen carriers in vertebrates, erythroid cells have evolved several mechanisms to efficiently transport and utilize iron within the cell for adequate heme synthesis. This is critical as mitochondrial iron import is tightly coupled with heme synthesis, and cells cannot preload iron in the mitochondria (64). In addition to the housekeeping mitochondrial iron importer MFRN2, erythroid cells express MFRN1 during their terminal maturation (22, 23). The tissue-restricted regulation at the transcriptional level for *MFRN1* at "erythroid super-enhancer" by GATA-factors (65, 66), is reminiscent of the transcriptional regulation of ALAS, the first and rate-limiting enzyme in the heme biosynthetic pathway (67). Like the *MFRN* genes, these *ALAS* genes are encoded by two separate genes, encoding distinct ALAS isoenzymes. The ubiq-

uitous *ALAS1* is regulated by heme via the peroxisome proliferator-activated 1α (PGC-1α) (68). The erythroid-enriched *ALAS2* and *MFRN1* genes are not regulated by heme. The post-translational regulation of ALAS2 is mediated by the intracellular levels of iron and iron-responsive protein 1 (IRP1) binding to its cognate iron-responsive element (IRE) in the 5′-untranslated region (UTR) of the *ALAS2* mRNA (69); however, no such regulation by iron on IRE have been reported and ascribed to the *MFRN* genes.

During terminal erythropoiesis, MFRN1 protein stability is also enhanced by oligomerization with ABCB10 (25, 26). MFRN1 and ABCB10 are in a physical complex with FECH, which kinetically favors the coupling of iron transport and heme synthesis. The addition of FAM210B, which forms an oligomer with PPOX and FECH to enhance mitochondrial iron import and heme synthesis, fits into this experimental model where FAM210B can nucleate or stabilize the formation of a complex between PPOX and FECH. In this manner, it can facilitate the transfer of PPIX to FECH and promote iron import coupled with heme synthesis (Fig. 7*D*). While PPOX and FECH physically interact, they do not form a tight complex. This supports the idea that bridging molecules, such as FAM210B, may mediate the strength of the interaction, hence modulating the rate of iron import and heme synthesis (70).

FAM210B plays a second role in heme synthesis by activating FECH enzymatic activity (Fig. 6, *D* and *E*). It is well-established that red cells increase the expression of ferrochelatase protein during erythropoiesis. This occurs either by increase in *FECH* mRNA transcription (71) or stabilization of FECH protein by binding of iron–sulfur clusters (72). In contrast, *FAM210B* deficiency does not alter FECH protein levels (Fig. 6*E*), suggesting that its effects on FECH activity may be mediated by the requirement for FAM210B for efficient iron delivery to FECH, and/or by playing a role in allosteric activation of the FECH enzyme. These data add to our understanding of the mechanisms by which Epo signaling regulates heme synthesis by post-translational regulation of FECH (49) and suggest mechanisms by which the activity of heme synthetic enzymes, in this case, FECH, may be rapidly modulated in response to metabolic requirements.

As *Fam210b* is also expressed in nondifferentiating erythroid cells and neural and hepatic tissues, it may also play a role in these tissues that is independent of heme synthesis and iron metabolism. Because FAM210B is a mitochondrial protein, detailed sequencing studies may reveal mutations in *FAM210B* that play a role in modifying the severity of mitochondriopathy in these tissues. Our identification of *Fam210b* as a novel mitochondrial protein that is required for optimal mitochondrial iron uptake during terminal erythropoiesis thus provides a novel genetic tool for further studies on vertebrate erythropoiesis and mitochondrial biology.

Materials and methods

Cell lines

MEL DS19 subclone cells were obtained from Arthur Skoultchi (Albert Einstein College of Medicine, New York). Human HEK293T cells were used for transient transfections.

GenBank™ accession numbers

Zebrafish *fam210b (c20orf108)* is GenBank™ accession number NM_001033751; mouse *Fam210b* is GenBank™ accession number NM_025912.

Knockdown of Dmt1 and Fam210b by shRNA hairpins in mouse cells

Dmt1 (GenBank™ accession number NM_008732.2) stable knockdown MEL clones were obtained by stable transfection of an shRNA hairpin, TRCN0000079535. *Fam210b* (GenBank™ accession number NM_025912) stable knockdown MEL clones were obtained by transfection of shRNA hairpins: shFam210b-1 and TRCN0000103732; shFam210b-2 TRCN0000103734. shRNA hairpins were obtained from Sigma. MEL clones were electroporated with shRNA plasmids by electroporation, and stable clones were obtained by limiting dilutions and selection with G418 (*Dmt1*).

CRISPR design and cloning

CRISPR guide sequences were designed to direct cleavages at genetic loci to generate chromosomal deletions (73, 74). CRISPR guide sequences were designed to have a unique 12-bp seed sequence 5′-NNNNNNNNNNNNGG-3′ in the mouse genome to minimize off-target cleavages. Exons 1 and 3 of the *Fam210b* locus were targeted. The exon 1 tgt1 targeting sequence was as follows: 5′-GCTCGCGGCGCGCCATGGCC-3′; exon 1 tgt2 targeting sequence was 5′-TCGGGCGTCCG-GAACCGGAT-3′, and the exon 3 targeting sequence was 5′-TACCGGGAGCAAACAGCTTATGGA-3′. Exons 2 and 4 of the *Mfrn1* locus were targeted. The exon 2 targeting sequence was as follows: 5′-GATGCTTGTATACCGGGCTT-3′; the exon 4 targeting sequence was 5′-GAAGAACTCATA-AACGGACC-3′. CRISPR guides were cloned into pX330 plasmid (Addgene) with BbsI ligation as described previously (75).

CRISPR/Cas9 genome editing in MEL cells

CRISPR/Cas9 constructs were delivered to MEL DS19 cells by electroporation. CRISPR/Cas9 constructs were co-electroporated with pEF1α at a 9:1 ratio. Two days later, cells were resuspended in puromycin media (5 μg/ml). Cells were plated by limiting dilution at 0.3 cells per well in 96-well plates and cultured at 37 °C. Clones were screened by gDNA isolation (QuickExtract, Epicenter), and PCR for the deletion allele (CRISPR 1), or PCR for the WT allele (CRISPR 2 and CRISPR 3). Clones were validated by Western blot analysis for FAM210B protein; *Mfrn1* gene expression was assayed by qRT-PCR (48).

The PCR primers to genotype *Fam210b* CRISPR 1 were as follows: mFam210b_F 5′-CTATAGAGCCCCGCCTATCC-3′ and mFam210b_R 5′-TCGGTCAGGTGCAATGTAAA-3′. The PCR primers used to genotype *Fam210b* CRISPR 2 and 3 were as follows: E3F 5′-GCATAGACATGTCTGCAATCC-3′ and E3R 5′-AGCCACCUUGCACACAGCCC-3′.

Iron radiolabeling and radio iron– heme measurements

$^{55}FeCl_3$ (specific activity: 1.28 Ci/mmol) (PerkinElmer Life Sciences) were loaded onto transferrin as described previously

(80). Metabolic labeling with ^{55}Fe-transferrin and quantitation of the incorporation of ^{55}Fe into heme were carried out as described previously (38).

ICP analysis of mitochondrial iron content

Mitochondrial iron was measured as described previously (76). Isolated mitochondria were treated with nitric acid, and sample iron content was determined by using an ICP optical emission spectrometer (PerkinElmer Life Sciences). The results were normalized to mitochondrial protein content.

HPLC analysis of heme and porphyrins

HPLC analysis was carried out with MEL cells that were differentiated for 72 h with 1.5% DMSO. A cell pellet spun down from a 30–50-ml culture was mixed with water to about 200 μl in a microcentrifuge tube and sonicated for 12 cycles with 5-s intervals at 50% duty (about 2.5 s on, 2.5 s off) using a microtip. A 50-μl aliquot was mixed vigorously with 200 μl of an extraction mixture of ethyl acetate (4 volumes) and glacial acetic acid (1 volume). The phases were separated by microcentrifugation for 1 min at maximum speed. The upper organic layer was immediately analyzed simultaneously for protoporphyrin IX and heme in the HPLC (38, 51).

Silencing of Fam210b in mouse primary fetal liver cells

Silencing of *Fam210b* and hemoglobin quantification in mouse primary fetal liver cells was carried out as described (77). The retroviral plasmids expressing shRNAs for *Fam210b* were transfected in a packaging HEK293T cell line. The collected retroviral supernatants were added to erythroid precursor cells purified from E14.5 mouse fetal liver (C57BL/6J). The retrovirally-transduced cells were sorted for GFP expression using a FACSAria machine (BD Biosciences), followed by *ex vivo* erythroid terminal development in Epo-only medium for 48 h. After culture, cells were collected for analysis on enucleation and hemoglobin content. The hemoglobin content was quantified with Drabkin's reagent used human hemoglobin as standards.

Fetal liver proliferation and enucleation assays

To measure proliferation rates, GFP-positive cells were plated in 24-well plates with a density at 100,000 cells/per ml, cultured in Epo-only erythroid differentiation medium. The number of cells was counted at the 24 and 48 h using a hemocytometer. In each time point, the cell numbers were the average of three biological samples, which were the average of two technical duplicates. To measure the rate of enucleations, after 48 h of culture, one million cells were spun down and resuspended with 100 μl of FACS buffer (PBS + 2% fetal bovine serum + 100 μM EDTA). Anti-Ter119 antibodies conjugated with APC (eBioscience) and Hoechst 33342 (Sigma) were added to stain the cells for 10 min at room temperature following manufacturer protocols. After staining, cells were washed with cold PBS twice and resuspended with the FACS buffer containing propidium iodide (Sigma) to distinguish between live and dead cells and were further analyzed on a FACS Fortessa machine. The details of protocols were previously described (78).

Functional complementation assays with chemicals in cultured cells

MEL cells were differentiated chemically with 2% DMSO for 72 h. For functional complementation assays with hinokitiol, cells were concurrently treated with 10 μM iron citrate and hinokitiol (1 μM) or C2dOHino (1 μM) (48). Chemical complementation with DP was carried out by treating cells with 5 μM DP (Frontier Scientific) as described (38).

Sub-mitochondrial localization studies

Crude mitochondria were isolated from MEL or primary fetal liver cells using a mitochondrial isolation kit (Pierce).

For mitochondrial sublocalization studies, MEL cells stably expressing mouse Fam210b were harvested at confluency and lysed in homogenization buffer (20 mM HEPES, pH 7.4, 220 mM mannitol, 70 mM sucrose) supplemented with 2 mg/ml BSA and 0.5 mM PMSF using a Teflon–Dounce homogenizer to release mitochondria. The lysates were centrifuged at 100 × *g* at 4 °C for 5 min. The post-nuclear supernatant was centrifuged at 10,000 × *g* for 10 min to obtain mitochondria pellets. The pellets were subsequently washed with homogenization buffer without BSA and PMSF, and mitochondria were collected by centrifugation. The protein concentration was measured using BCA assay according to the vendor's protocols (ThermoFisher Scientific).

For mitochondrial fractionation, mitochondria (equivalent of 50 μg of mitochondrial protein per reaction) were suspended in homogenization buffer, 20 mM HEPES (for osmotic shock) or 20 mM HEPES with 1% Triton X-100 in the presence or absence of 5 μg/ml proteinase K for 30 min at 4 °C. Proteinase K was inactivated with the addition of 1 mM PMSF. Samples were centrifuged at 10,000 × *g* at 4 °C to obtain the pellet that contained mitoplasts (the matrix and inner membrane). The supernatant was collected and precipitated with trichloroacetic acid (TCA, final concentration of 15% TCA) to obtain soluble proteins. The proteins (50 μg per lane) were separated by SDS-PAGE followed by immunoblot analysis.

Mitochondria (equivalent of 50 μg of mitochondrial protein per reaction) were suspended in homogenization buffer or 0.1 M sodium carbonate, pH 11.5, for 30 min at 4 °C. Then, the samples were centrifuged at 28,000 × *g* for 30 min at 4 °C to obtain the pellet of precipitated membrane proteins. The supernatant with soluble proteins was TCA-precipitated. The proteins (50 μg per lane) were separated by SDS-PAGE followed by immunoblot analysis.

Western blot analysis

The following antibodies were used in this study: TIMM23 (BD Biosciences catalog no. 611222); TOMM20 (Santa Cruz Biotechnology clone FL-145); Mortalin (Proteintech catalog no. 1488-14-AP).PreP and Yme1L polyclonal antibodies were raised against recombinant proteins (Pacific Immunology). Immunoblotting of FAM210B was performed using a custom anti-mouse FAM210B polyclonal antibody generated against three peptides (C-LSHPVPDARLLRTARGDC, C-TGTEK-

KLSRTQQLKKVC, and C-KLGFKESLVQSKMAC), and immunoaffinity-purified against these antigenic peptides (Genemed Synthesis, Inc., San Antonio, TX). Anti-FECH polyclonal (C-20), HA (Y-11), hemoglobin a (H-80), and HSP60 (K-19) antibodies were obtained from Santa Cruz Biotechnology (Athens, GA). Anti-TFRC (H68.4) was obtained from Invitrogen. Anti-GAPDH was obtained from Pierce (GA1R). Anti-FLAG M2-HRP was obtained from Sigma (catalog no. A8592). HSP90 antibody was obtained from Cell Signaling (C45G5). For Fig. 7*C*, we used anti-FECH polyclonal antibodies from Kerafast (EGA191).

qRT-PCR

qRT-PCR probes were obtained from Invitrogen. Murine *Fam210b* probe is Mm00508881_m1; *Hprt* probe is Mm01545399_m1. Zebrafish *fam210b* probe is Dr03426307_m1; *hprt* probe is Dr03138604_m1. The mouse tissue cDNA array was purchased from Clontech.

Chemical hinokitiol and functional complementation in zebrafish

24-hpf morphant embryos in the transgenic *Tg*(*globinLCR:eGFP*) line were dechorionated with Pronase as described (54) and incubated in the presence of 1 μM hinokitiol + 10 μM iron citrate for another 48 h (48). For specificity, the control, inactive C2 deoxyhinokitiol was 1 μM final concentration with iron citrate. Vehicle-treated embryos were exposed to 0.01 mM DMSO. Control or morphant embryos at roughly 72 hpf were mechanically homogenized as described previously for flow cytometry (45, 54).

Genetic complementation assays

Genetic complementation of the Δ*mrs3/4* yeast strain with chimeric vertebrate Fam210b and Mfrn1, containing the first N-terminal 23 amino acid residues from yeast Mrs3 subcloned in the pRS426-ADH vector, was performed as described previously (23). Western blot analysis of the total, mitochondrial, and cytosolic fraction was described previously with anti-FLAG and anti-porin antibodies.

Control and *Mfrn2*$^{-/-}$ mouse embryonic fibroblasts (MEF) were isolated from the skin of 3-month-old mice and immortalized by forcing through a senescence crisis. Mfrn2-GFP or Fam210b-HA was transiently expressed in these MEF cells. Transfected MEF cells were treated with DFO (10–50 μM). Cellular viability was then assayed using a cell titer blue assay, which measures conversion of resazurin to resorufin on a 96-well format (Promega).

Immunoprecipitation of FAM210B and its interacting proteins

CPOX-FLAG, PPOX-FLAG, FECH-FLAG, and *FAM210B-HA* were cloned into the pEF1 vector and expressed under the control of the EF1 promoter. pEF1/FAM210B-HA was co-transfected with pEF1 empty vector, pEF1/CPOX-FLAG, pEF1/PPOX-FLAG, or pEF1/FECH-FLAG into 10-cm^3 dishes of HEK293T cells using a Lipofectamine 2000 reagent-based method (Invitrogen). Cells were harvested 48 h post-transfection and lysed in a buffer containing 1% Nonidet P-40, 300 mM NaCl, 50 mM Tris, pH 8.0, and protease inhibitor mixture (Pierce). Cell lysates were precleared with mouse IgG-agarose (Sigma) for 60 min at 4 °C. Precleared lysates were then incubated with anti-FLAG or anti-HA–agarose beads (Sigma) for 2 h at 4 °C. Beads were washed three times for 15 min in lysis buffer. Immunoprecipitated proteins were subsequently eluted with Laemmli buffer and resolved by SDS-PAGE.

To determine whether FAM210B interacted with endogenous FECH, we electroporated pEF1/FAM210B-FLAG into MEL cells and selected FAM210B-FLAG expressing single cell clones by limiting dilution. pEF1/FAM210B-HA and pEF1 empty vector expressing cell lines were differentiated with 1.5% DMSO for 72 h. For each immunoprecipitation experiment, we lysed 100 million differentiated cells with 1 ml of lysis buffer (77). 2 mg of protein was used as the starting material for each immunoprecipitation sample. Samples were precleared with mouse IgG beads and immunoprecipitated with anti-FLAG M2–agarose for 4 h at 4 °C. Beads were washed three times for 15 min at 4 °C. Proteins were eluted with Laemmli buffer, resolved by SDS-PAGE, and analyzed by Western blotting.

Statistics

Statistical analysis was carried out using two-tailed paired or unpaired Student's *t* test. Significance was set at $p < 0.05$. All data points were plotted as scatter plots, representing all replicates of each experiment.

Study approval

All zebrafish experiments were performed in accordance with the Institutional Animal Care and Use Committee (IACUC) regulations of Brigham and Women's Hospital. WT AB zebrafish were used for all zebrafish experiments. All mouse experiments were performed in accordance with IACUC regulations at the Massachusetts Institute of Technology and University of Utah.

Author contributions—Y. Y. Y., J. S., C. C., D. E. B., C. M. K., D. M. W., H. F. L., and B. H. P. conceptualization; Y. Y. Y. and B. H. P. resources; Y. Y. Y., J. S., C. C., J. T. C., A. S. G., R. S., L. L., M. D. K., P. D. K., M. J. K., J. P., D. E. B., C. M. K., J. D. P., J. K., D. M. W., and B. H. P. data curation; Y. Y. Y., J. S., C. C., J. T. C., A. S. G., R. S., L. L., M. D. K., P. D. K., M. J. K., M. D. B., D. E. B., S. H. O., C. M. K., J. D. P., J. K., D. M. W., H. F. L., and B. H. P. formal analysis; Y. Y. Y., C. C., J. P., M. D. B., D. E. B., S. H. O., C. M. K., J. D. P., J. K., D. M. W., H. F. L., and B. H. P. supervision; Y. Y. Y., C. C., L. Z., J. P., M. D. B., D. E. B., S. H. O., C. M. K., J. D. P., J. K., D. M. W., H. F. L., and B. H. P. funding acquisition; Y. Y. Y., J. S., C. C., C. M. K., and D. M. W. validation; Y. Y. Y., J. S., C. C., J. T. C., A. S. G., R. S., L. L., X. Z., M. D. B., C. M. K., J. D. P., J. K., D. M. W., H. F. L., and B. H. P. investigation; Y. Y. Y., J. S., C. C., A. S. G., R. S., L. L., X. Z., J. A., H. L., L. Z., D. E. B., S. H. O., C. M. K., D. M. W., and B. H. P. methodology; Y. Y. Y., J. S., P. D. K., C. M. K., D. M. W., and B. H. P. writing-original draft; Y. Y. Y., M. D. B., D. E. B., C. M. K., J. D. P., J. K., D. M. W., H. F. L., and B. H. P. project administration; Y. Y. Y., J. S., C. C., J. T. C., A. S. G., R. S., L. L., M. D. K., M. J. K., J. A., L. Z., J. P., M. D. B., D. E. B., S. H. O., C. M. K., J. D. P., J. K., D. M. W., H. F. L., and B. H. P. writing-review and editing.

Acknowledgments—We thank Iman Schultz for assistance on bioinformatics analysis, Johannes Wittig for assistance with model figure preparation, and Nicholas Huston for assistance with initial morpholino injections. We thank Mahnaz Paktinat for training on the use of the BD FACSCanto cell sorter. We also thank Bingbing Yuan for help with processing and analyzing the microarray data. The DS19 MEL clones were obtained from Arthur Skoultchi (Albert Einstein College of Medicine). We thank Eva Buys and her crew for the zebrafish animal husbandry. We also thank Harry Dailey and Amy Medlock for their critical feedback on the manuscript and Stashauna Carter for technical assistance. Fluorescence confocal microscopy was performed at the Harvard Digestive Disease Center Imaging Facility (Boston Children's Hospital, supported by National Institutes of Health Grant P30 DK34854) with assistance from Ramiro Massol. HPLC analyses of porphyrins were performed at the University of Utah Center for Iron and Heme Disorders supported by National Institutes of Health Grant U54 DK110858.

References

1. Richmond, T. D., Chohan, M., and Barber, D. L. (2005) Turning cells red: signal transduction mediated by erythropoietin. *Trends Cell Biol.* **15,** 146–155 CrossRef Medline
2. Gammella, E., Diaz, V., Recalcati, S., Buratti, P., Samaja, M., Dey, S., Noguchi, C. T., Gassmann, M., and Cairo, G. (2015) Erythropoietin's inhibiting impact on hepcidin expression occurs indirectly. *Am. J. Physiol. Regul. Integr. Comp. Physiol.* **308,** R330–R335 CrossRef Medline
3. Nai, A., Rubio, A., Campanella, A., Gourbeyre, O., Artuso, I., Bordini, J., Gineste, A., Latour, C., Besson-Fournier, C., Lin, H. Y., Coppin, H., Roth, M.-P., Camaschella, C., Silvestri, L., Meynard, D., Franke, K., *et al.* (2016) Limiting hepatic Bmp-Smad signaling by matriptase-2 is required for erythropoietin-mediated hepcidin suppression in mice. *Blood* **127,** 99–101 Medline CrossRef
4. Feng, D., and Lazar, M. A. (2012) Clocks, metabolism, and the epigenome. *Mol. Cell* **47,** 158–167 CrossRef Medline
5. Girvan, H. M., and Munro, A. W. (2013) Heme sensor proteins. *J. Biol. Chem.* **288,** 13194–13203 CrossRef Medline
6. Maio, N., and Rouault, T. A. (2015) Iron–sulfur cluster biogenesis in mammalian cells: new insights into the molecular mechanisms of cluster delivery. *Biochim. Biophys. Acta* **1853,** 1493–512 CrossRef Medline
7. Martínková, M., Kitanishi, K., and Shimizu, T. (2013) Heme-based globin-coupled oxygen sensors: linking oxygen binding to functional regulation of diguanylate cyclase, histidine kinase, and methyl-accepting chemotaxis. *J. Biol. Chem.* **288,** 27702–27711 CrossRef Medline
8. Matak, P., Matak, A., Moustafa, S., Aryal, D. K., Benner, E. J., Wetsel, W., and Andrews, N. C. (2016) Disrupted iron homeostasis causes dopaminergic neurodegeneration in mice. *Proc. Natl. Acad. Sci. U.S.A.* **113,** 3428–3435 CrossRef Medline
9. Ramsey, A. J., Hillas, P. J., and Fitzpatrick, P. F. (1996) Characterization of the active site iron in tyrosine hydroxylase. *J. Biol. Chem.* **271,** 24395–24400 CrossRef Medline
10. Andrews, N. C. (2008) Forging a field: the golden age of iron biology. *Blood* **112,** 219–230 CrossRef Medline
11. Chen, C., and Paw, B. H. (2012) Cellular and mitochondrial iron homeostasis in vertebrates. *Biochim. Biophys. Acta* **1823,** 1459–1467 CrossRef Medline
12. Philpott, C. C., Leidgens, S., and Frey, A. G. (2012) Metabolic remodeling in iron-deficient fungi. *Biochim. Biophys. Acta* **1823,** 1509–1520 CrossRef Medline
13. Hentze, M. W., Muckenthaler, M. U., and Andrews, N. C. (2004) Balancing acts. *Cell* **117,** 285–297 CrossRef Medline
14. Levy, J. E., Jin, O., Fujiwara, Y., Kuo, F., and Andrews, N. C. (1999) Transferrin receptor is necessary for development of erythrocytes and the nervous system. *Nat. Genet.* **21,** 396–399 CrossRef Medline
15. Chen, C., Garcia-Santos, D., Ishikawa, Y., Seguin, A., Li, L., Fegan, K. H., Hildick-Smith, G. J., Shah, D. I., Cooney, J. D., Chen, W., King, M. J., Yien, Y. Y., Schultz, I. J., Anderson, H., Dalton, A. J., *et al.* (2013) Snx3 regulates recycling of the transferrin receptor and iron assimilation. *Cell Metab.* **17,** 343–352 CrossRef Medline
16. Lim, J. E., Jin, O., Bennett, C., Morgan, K., Wang, F., Trenor, C. C., 3rd., Fleming, M. D., and Andrews, N. C. (2005) A mutation in Sec15l1 causes anemia in hemoglobin deficit (hbd) mice. *Nat. Genet.* **37,** 1270–1273 CrossRef Medline
17. Ohgami, R. S., Campagna, D. R., Greer, E. L., Antiochos, B., McDonald, A., Chen, J., Sharp, J. J., Fujiwara, Y., Barker, J. E., and Fleming, M. D. (2005) Identification of a ferrireductase required for efficient transferrin-dependent iron uptake in erythroid cells. *Nat. Genet.* **37,** 1264–1269 CrossRef Medline
18. Fleming, M. D., Romano, M. A., Su, M. A., Garrick, L. M., Garrick, M. D., and Andrews, N. C. (1998) Nramp2 is mutated in the anemic Belgrade (b) rat: evidence of a role for Nramp2 in endosomal iron transport. *Proc. Natl. Acad. Sci. U.S.A.* **95,** 1148–1153 CrossRef Medline
19. Fleming, M. D., Trenor, C. C., 3rd., Su, M. A., Foernzler, D., Beier, D. R., Dietrich, W. F., and Andrews, N. C. (1997) Microcytic anaemia mice have a mutation in Nramp2, a candidate iron transporter gene. *Nat. Genet.* **16,** 383–386 CrossRef Medline
20. Gunshin, H., Mackenzie, B., Berger, U. V., Gunshin, Y., Romero, M. F., Boron, W. F., Nussberger, S., Gollan, J. L., and Hediger, M. A. (1997) Cloning and characterization of a mammalian proton-coupled metal-ion transporter. *Nature* **388,** 482–488 CrossRef Medline
21. Wolff, N. A., Ghio, A. J., Garrick, L. M., Garrick, M. D., Zhao, L., Fenton, R. A., and Thévenod, F. (2014) Evidence for mitochondrial localization of divalent metal transporter 1 (DMT1). *FASEB J.* **28,** 2134–2145 CrossRef Medline
22. Paradkar, P. N., Zumbrennen, K. B., Paw, B. H., Ward, D. M., and Kaplan, J. (2009) Regulation of mitochondrial iron import through differential turnover of mitoferrin 1 and mitoferrin 2. *Mol. Cell. Biol.* **29,** 1007–1016 CrossRef Medline
23. Shaw, G. C., Cope, J. J., Li, L., Corson, K., Hersey, C., Ackermann, G. E., Gwynn, B., Lambert, A. J., Wingert, R. A., Traver, D., Trede, N. S., Barut, B. A., Zhou, Y., Minet, E., Donovan, A., *et al.* (2006) Mitoferrin is essential for erythroid iron assimilation. *Nature* **440,** 96–100 CrossRef Medline
24. Christenson, E. T., Gallegos, A. S., and Banerjee, A. (2018) *In vitro* reconstitution, functional dissection, and mutational analysis of metal ion transport by mitoferrin-1. *J. Biol. Chem.* **293,** 3819–3828 CrossRef Medline
25. Chen, W., Paradkar, P. N., Li, L., Pierce, E. L., Langer, N. B., Takahashi-Makise, N., Hyde, B. B., Shirihai, O. S., Ward, D. M., Kaplan, J., and Paw, B. H. (2009) Abcb10 physically interacts with mitoferrin-1 (Slc25a37) to enhance its stability and function in the erythroid mitochondria. *Proc. Natl. Acad. Sci. U.S.A.* **106,** 16263–16268 CrossRef Medline
26. Chen, W., Dailey, H. A., and Paw, B. H. (2010) Ferrochelatase forms an oligomeric complex with mitoferrin-1 and Abcb10 for erythroid heme biosynthesis. *Blood* **116,** 628–630 CrossRef Medline
27. Froschauer, E. M., Rietzschel, N., Hassler, M. R., Binder, M., Schweyen, R. J., Lill, R., Mühlenhoff, U., and Wiesenberger, G. (2013) The mitochondrial carrier Rim2 co-imports pyrimidine nucleotides and iron. *Biochem. J.* **455,** 57–65 CrossRef Medline
28. Mühlenhoff, U., Stadler, J. A., Richhardt, N., Seubert, A., Eickhorst, T., Schweyen, R. J., Lill, R., and Wiesenberger, G. (2003) A specific role of the yeast mitochondrial carriers Mrs3/4p in mitochondrial iron acquisition under iron-limiting conditions. *J. Biol. Chem.* **278,** 40612–40620 CrossRef Medline
29. Kondo, A., Fujiwara, T., Okitsu, Y., Fukuhara, N., Onishi, Y., Nakamura, Y., Sawada, K., and Harigae, H. (2016) Identification of a novel putative mitochondrial protein FAM210B associated with erythroid differentiation. *Int. J. Hematol.* **103,** 387–395 CrossRef Medline
30. Sun, S., Liu, J., Zhao, M., Han, Y., Chen, P., Mo, Q., Wang, B., Chen, G., Fang, Y., Tian, Y., Zhou, J., Ma, D., Gao, Q., and Wu, P. (2017) Loss of the novel mitochondrial protein FAM210B promotes metastasis via PDK4-dependent metabolic reprogramming. *Cell Death Dis.* **8,** e2870 CrossRef Medline

31. Napier, I., Ponka, P., and Richardson, D. R. (2005) Iron trafficking in the mitochondrion: novel pathways revealed by disease. *Blood* **105,** 1867–1874 CrossRef Medline
32. Richardson, D. R., Lane, D. J., Becker, E. M., Huang, M. L., Whitnall, M., Suryo Rahmanto, Y., Sheftel, A. D., and Ponka, P. (2010) Mitochondrial iron trafficking and the integration of iron metabolism between the mitochondrion and cytosol. *Proc. Natl. Acad. Sci. U.S.A.* **107,** 10775–10782 CrossRef Medline
33. Lu, X., Huang, L. J., and Lodish, H. F. (2008) Dimerization by a cytokine receptor is necessary for constitutive activation of JAK2V617F. *J. Biol. Chem.* **283,** 5258–5266 CrossRef Medline
34. Wong, P., Hattangadi, S. M., Cheng, A. W., Frampton, G. M., Young, R. A., and Lodish, H. F. (2011) Gene induction and repression during terminal erythropoiesis are mediated by distinct epigenetic changes. *Blood* **118,** e128–38 CrossRef Medline
35. Socolovsky, M., Fallon, A. E., Wang, S., Brugnara, C., and Lodish, H. F. (1999) Fetal anemia and apoptosis of red cell progenitors in Stat5a(−/−)5b(−/−) mice: a direct role for stat5 in Bcl-X(L) induction. *Cell* **98,** 181–191 CrossRef Medline
36. Schneider-Poetsch, T., Ju, J., Eyler, D. E., Dang, Y., Bhat, S., Merrick, W. C., Green, R., Shen, B., and Liu, J. O. (2010) Inhibition of eukaryotic translation elongation by cycloheximide and lactimidomycin. *Nat. Chem. Biol.* **6,** 209–217 CrossRef Medline
37. Chung, J., Bauer, D. E., Ghamari, A., Nizzi, C. P., Deck, K. M., Kingsley, P. D., Yien, Y. Y., Huston, N. C., Chen, C., Schultz, I. J., Dalton, A. J., Wittig, J. G., Palis, J., Orkin, S. H., Lodish, H. F., *et al.* (2015) The mTORC1/4E-BP pathway coordinates hemoglobin production with L-leucine availability. *Sci. Signal.* **8,** ra34 CrossRef Medline
38. Yien, Y. Y., Robledo, R. F., Schultz, I. J., Takahashi-Makise, N., Gwynn, B., Bauer, D. E., Dass, A., Yi, G., Li, L., Hildick-Smith, G. J., Cooney, J. D., Pierce, E. L., Mohler, K., Dailey, T. A., Miyata, N., *et al.* (2014) TMEM14C is required for erythroid mitochondrial heme metabolism. *J. Clin. Invest.* **124,** 4294–4304 CrossRef Medline
39. Zhang, J., Socolovsky, M., Gross, A. W., and Lodish, H. F. (2003) Role of Ras signaling in erythroid differentiation of mouse fetal liver cells: functional analysis by a flow cytometry-based novel culture system. *Blood* **102,** 3938–3946 CrossRef Medline
40. Kingsley, P. D., Greenfest-Allen, E., Frame, J. M., Bushnell, T. P., Malik, J., McGrath, K. E., Stoeckert, C. J., and Palis, J. (2013) Ontogeny of erythroid gene expression. *Blood* **121,** e5-e13 CrossRef Medline
41. Metzendorf, C., and Lind, M. I. (2010) *Drosophila* mitoferrin is essential for male fertility: evidence for a role of mitochondrial iron metabolism during spermatogenesis. *BMC Dev. Biol.* **10,** 68 CrossRef Medline
42. Stainier, D. Y., Weinstein, B. M., Detrich, H. W., 3rd., Zon, L. I., and Fishman, M. C. (1995) Cloche, an early acting zebrafish gene, is required by both the endothelial and hematopoietic lineages. *Development* **121,** 3141–3150 Medline
43. Reischauer, S., Stone, O. A., Villasenor, A., Chi, N., Jin, S.-W., Martin, M., Lee, M. T., Fukuda, N., Marass, M., Witty, A., Fiddes, I., Kuo, T., Chung, W.-S., Salek, S., Lerrigo, R., *et al.* (2016) Cloche is a bHLH-PAS transcription factor that drives haemato-vascular specification. *Nature* **535,** 294–298 CrossRef Medline
44. Hammerschmidt, M., Pelegri, F., Mullins, M. C., Kane, D. A., van Eeden, F. J., Granato, M., Brand, M., Furutani-Seiki, M., Haffter, P., Heisenberg, C. P., Jiang, Y. J., Kelsh, R. N., Odenthal, J., Warga, R. M., and Nüsslein-Volhard, C. (1996) Dino and mercedes, two genes regulating dorsal development in the zebrafish embryo. *Development* **123,** 95–102 Medline
45. Ganis, J. J., Hsia, N., Trompouki, E., de Jong, J. L., DiBiase, A., Lambert, J. S., Jia, Z., Sabo, P. J., Weaver, M., Sandstrom, R., Stamatoyannopoulos, J. A., Zhou, Y., and Zon, L. I. (2012) Zebrafish globin switching occurs in two developmental stages and is controlled by the LCR. *Dev. Biol.* **366,** 185–194 CrossRef Medline
46. Fujiki, Y., Hubbard, A. L., Fowler, S., and Lazarow, P. B. (1982) Isolation of intracellular membranes by means of sodium carbonate treatment: application to endoplasmic reticulum. *J. Cell Biol.* **93,** 97–102 CrossRef Medline
47. Ye, H., and Rouault, T. A. (2010) Human iron–sulfur cluster assembly, cellular iron homeostasis, and disease. *Biochemistry* **49,** 4945–4956 CrossRef Medline
48. Grillo, A. S., SantaMaria, A. M., Kafina, M. D., Cioffi, A. G., Huston, N. C., Han, M., Seo, Y. A., Yien, Y. Y., Nardone, C., Menon, A. V., Fan, J., Svoboda, D. C., Anderson, J. B., Hong, J. D., Nicolau, B. G., *et al.* (2017) A small-molecule iron transporter restores hemoglobinization in protein-deficient animals. *Science* **356,** 608–616 Medline
49. Chung, J., Wittig, J. G., Ghamari, A., Maeda, M., Dailey, T. A., Bergonia, H., Kafina, M. D., Coughlin, E. E., Minogue, C. E., Hebert, A. S., Li, L., Kaplan, J., Lodish, H. F., Bauer, D. E., Orkin, S. H., *et al.* (2017) Erythropoietin signaling regulates heme biosynthesis. *Elife* CrossRef Medline
50. Dailey, H. A., and Fleming, J. E. (1983) Bovine ferrochelatase. Kinetic analysis of inhibition by *N*-methylprotoporphyrin, manganese, and heme. *J. Biol. Chem.* **258,** 11453–11459 Medline
51. Troadec, M. B., Warner, D., Wallace, J., Thomas, K., Spangrude, G. J., Phillips, J., Khalimonchuk, O., Paw, B. H., Ward, D. M., and Kaplan, J. (2011) Targeted deletion of the mouse Mitoferrin1 gene: From anemia to protoporphyria. *Blood* **117,** 5494–5502 CrossRef Medline
52. Chung, J., Anderson, S. A., Gwynn, B., Deck, K. M., Chen, M. J., Langer, N. B., Shaw, G. C., Huston, N. C., Boyer, L. F., Datta, S., Paradkar, P. N., Li, L., Wei, Z., Lambert, A. J., Sahr, K., *et al.* (2014) Iron regulatory protein-1 protects against mitoferrin-1-deficient porphyria. *J. Biol. Chem.* **289,** 7835–7843 CrossRef Medline
53. Wingert, R. A., Galloway, J. L., Barut, B., Foott, H., Fraenkel, P., Axe, J. L., Weber, G. J., Dooley, K., Davidson, A. J., Schmidt, B., Paw, B. H., Shaw, G. C., Kingsley, P., Palis, J., Schubert, H., *et al.* (2005) Deficiency of glutaredoxin 5 reveals Fe-S clusters are required for vertebrate haem synthesis. *Nature* **436,** 1035–1039 CrossRef Medline
54. Kardon, J. R., Yien, Y. Y., Huston, N. C., Branco, D. S., Hildick-Smith, G. J., Rhee, K. Y., Paw, B. H., and Baker, T. A. (2015) Mitochondrial ClpX activates a key enzyme for heme biosynthesis and erythropoiesis. *Cell* **161,** 858–867 CrossRef Medline
55. Cioffi, A. G., Hou, J., Grillo, A. S., Diaz, K. A., Burke, M. D. (2015) Restored physiology in protein-deficient yeast by a small-molecule channel. *J. Am. Chem. Soc.* **137,** 10096–10099 CrossRef Medline
56. Yu, M., Riva, L., Xie, H., Schindler, Y., Moran, T. B., Cheng, Y., Yu, D., Hardison, R., Weiss, M. J., Orkin, S. H., Bernstein, B. E., Fraenkel, E., and Cantor, A. B. (2009) Insights into GATA-1-mediated gene activation versus repression via genome-wide chromatin occupancy analysis. *Mol. Cell* **36,** 682–695 CrossRef Medline
57. Chami, N., Chen, M.-H., Slater, A. J., Eicher, J. D., Evangelou, E., Tajuddin, S. M., Love-Gregory, L., Kacprowski, T., Schick, U. M., Nomura, A., Giri, A., Lessard, S., Brody, J. A., Schurmann, C., Pankratz, N., *et al.* (2016) Exome genotyping identifies pleiotropic variants associated with red blood cell traits. *Am. J. Hum. Genet.* **99,** 8–21 CrossRef Medline
58. Ganesh, S. K., Zakai, N. A., van Rooij, F. J., Soranzo, N., Smith, A. V., Nalls, M. A., Chen, M.-H., Kottgen, A., Glazer, N. L., Dehghan, A., Kuhnel, B., Aspelund, T., Yang, Q., Tanaka, T., Jaffe, A., *et al.* (2009) Multiple loci influence erythrocyte phenotypes in the CHARGE Consortium. *Nat. Genet.* **41,** 1191–1198 CrossRef Medline
59. Hindorff, L. A., Sethupathy, P., Junkins, H. A., Ramos, E. M., Mehta, J. P., Collins, F. S., and Manolio, T. A. (2009) Potential etiologic and functional implications of genome-wide association loci for human diseases and traits. *Proc. Natl. Acad. Sci. U.S.A.* **106,** 9362–9367 CrossRef Medline
60. Soranzo, N., Spector, T. D., Mangino, M., Kühnel, B., Rendon, A., Teumer, A., Willenborg, C., Wright, B., Chen, L., Li, M., Salo, P., Voight, B. F., Burns, P., Laskowski, R. A., Xue, Y., *et al.* (2009) A genome-wide meta-analysis identifies 22 loci associated with eight hematological parameters in the HaemGen consortium. *Nat. Genet.* **41,** 1182–1190 CrossRef Medline
61. Ulirsch, J. C., Nandakumar, S. K., Wang, L., Giani, F. C., Zhang, X., Rogov, P., Melnikov, A., McDonel, P., Do, R., Mikkelsen, T. S., and Sankaran, V. G. (2016) Systematic functional dissection of common genetic variation affecting red blood cell traits. *Cell* **165,** 1530–1545 CrossRef Medline
62. Wang, Y., Langer, N. B., Shaw, G. C., Yang, G., Li, L., Kaplan, J., Paw, B. H., and Bloomer, J. R. (2011) Abnormal mitoferrin-1 expression in patients

with erythropoietic protoporphyria. *Exp. Hematol.* **39,** 784–794 CrossRef Medline

63. Visconte, V., Avishai, N., Mahfouz, R., Tabarroki, A., Cowen, J., Sharghi-Moshtaghin, R., Hitomi, M., Rogers, H. J., Hasrouni, E., Phillips, J., Sekeres, M. A., Heuer, A. H., Sauntharajah, Y., Barnard, J., and Tiu, R. V. (2015) Distinct iron architecture in SF3B1 mutant myelodysplastic syndromes patients is linked to an SLC25A37 splice variant with a retained intron. *Leukemia* **29,** 188–195 Medline
64. Lange, H., Kispal, G., and Lill, R. (1999) Mechanism of iron transport to the site of heme synthesis inside yeast mitochondria. *J. Biol. Chem.* **274,** 18989–18996 CrossRef Medline
65. Amigo, J. D., Yu, M., Troadec, M.-B., Gwynn, B., Cooney, J. D., Lambert, A. J., Chi, N. C., Weiss, M. J., Peters, L. L., Kaplan, J., Cantor, A. B., and Paw, B. H. (2011) Identification of distal cis-regulatory elements at mouse mitoferrin loci using zebrafish transgenesis. *Mol. Cell Biol.* **31,** 1344–1356 CrossRef Medline
66. Huang, J., Liu, X., Li, D., Shao, Z., Cao, H., Zhang, Y., Trompouki, E., Bowman, T. V., Zon, L. I., Yuan, G.-C., Orkin, S. H., and Xu, J. (2016) Dynamic control of enhancer repertoires drives lineage and stage-specific transcription during hematopoiesis. *Dev. Cell* **36,** 9–23 CrossRef Medline
67. Surinya, K. H., Cox, T. C., and May, B. K. (1997) Transcriptional regulation of the human erythroid 5-aminolevulinate synthase gene. Identification of promoter elements and role of regulatory proteins. *J. Biol. Chem.* **272,** 26585–26594 CrossRef Medline
68. Handschin, C., Lin, J., Rhee, J., Peyer, A. K., Chin, S., Wu, P. H., Meyer, U. A., and Spiegelman, B. M. (2005) Nutritional regulation of hepatic heme biosynthesis and porphyria through PGC-1α. *Cell* **122,** 505–515 CrossRef Medline
69. Cox, T. C., Bawden, M. J., Martin, A., and May, B. K. (1991) Human erythroid 5-aminolevulinate synthase: promoter analysis and identification of an iron-responsive element in the mRNA. *EMBO J.* **10,** 1891–1902 CrossRef Medline
70. Proulx, K. L., Woodard, S. I., and Dailey, H. A. (1993) *In situ* conversion of coproporphyrinogen to heme by murine mitochondria: terminal steps of the heme biosynthetic pathway. *Protein Sci.* **2,** 1092–1098 CrossRef Medline
71. Ning, B., Liu, G., Liu, Y., Su, X., Anderson, G. J., Zheng, X., Chang, Y., Guo, M., Liu, Y., Zhao, Y., and Nie, G. (2011) 5-Aza-2′-deoxycytidine activates iron uptake and heme biosynthesis by increasing c-Myc nuclear localization and binding to the E-boxes of transferrin receptor 1 (TfR1) and ferrochelatase (Fech) genes. *J. Biol. Chem.* **286,** 37196–37206 CrossRef Medline
72. Crooks, D. R., Ghosh, M. C., Haller, R. G., Tong, W. H., and Rouault, T. A. (2010) Posttranslational stability of the heme biosynthetic enzyme ferrochelatase is dependent on iron availability and intact iron–sulfur cluster assembly machinery. *Blood* **115,** 860–869 CrossRef Medline
73. Canver, M. C., Bauer, D. E., Dass, A., Yien, Y. Y., Chung, J., Masuda, T., Maeda, T., Paw, B. H., and Orkin, S. H. (2014) Characterization of genomic deletion efficiency mediated by CRISPR/Cas9 in mammalian cells. *J. Biol. Chem.* **289,** 21312–21324 CrossRef Medline
74. Cong, L., Ran, F. A., Cox, D., Lin, S., Barretto, R., Habib, N., Hsu, P. D., Wu, X., Jiang, W., Marraffini, L. A., and Zhang, F. (2013) Multiplex genome engineering using CRISPR/Cas systems. *Science* **339,** 819–823 CrossRef Medline
75. Ran, F. A., Hsu, P. D., Wright, J., Agarwala, V., Scott, D. A., and Zhang, F. (2013) Genome engineering using the CRISPR-Cas9 system. *Nat. Protoc.* **8,** 2281–2308 CrossRef Medline
76. Li, L., Chen, O. S., McVey Ward, D., and Kaplan, J. (2001) CCC1 is a transporter that mediates vacuolar iron storage in yeast. *J. Biol. Chem.* **276,** 29515–29519 CrossRef Medline
77. Hattangadi, S. M., Burke, K. A., and Lodish, H. F. (2010) Homeodomain-interacting protein kinase 2 plays an important role in normal terminal erythroid differentiation. *Blood* **115,** 4853–4861 CrossRef Medline
78. Cheng, A. W., Shi, J., Wong, P., Luo, K. L., Trepman, P., Wang, E. T., Choi, H., Burge, C. B., and Lodish, H. F. (2014) Muscleblind-like 1 (Mbnl1) regulates pre-mRNA alternative splicing during terminal erythropoiesis. *Blood* **124,** 598–610 CrossRef Medline
79. Medlock, A. E., Shiferaw, M. T., Marcero, J. R., Vashisht, A. A., Wohlschlegel, J. A., Phillips, J. D., and Dailey, H. A. (2015) Identification of the mitochondrial heme metabolism complex. *PLoS One* e0135896 CrossRef Medline
80. Roy, C. N., Penny, D. M., Feder, J. N., and Enns, C. A. (1999) The hereditary hemochromatosis protein, HFE, specifically regulates transferrin-mediated iron uptake in HeLa cells. *J. Biol. Chem.* **274,** 9022–9028 CrossRef Medline
81. Rossi, E., Costin, K.A., and Garcia-Webb, P. (1988) Ferrochelatase activity in human lymphocytes, as quantified by a new high-performance liquid-chromatographic method. *Clin. Chem.* **34,** 2481–2485 Medline